CP asymmetry from the effect of isospin symmetry breaking during B-meson decay*

Wan-Ying Yao (姚琬颖)[1†] Gang Lü (吕刚)[1‡] Xin-Heng Guo (郭新恒)[2§] Hai-Feng Ou (欧海峰)[1♮]

[1]Institute of Theoretical Physics, College of Physics, Henan University of Technology, Zhengzhou 450001, China
[2]College of Nuclear Science and Technology, Beijing Normal University, Beijing 100875, China

Abstract: The direct CP asymmetry in quasi-two-body decays of $B\to(V\to\pi^+\pi^-)P$ is investigated using the perturbative QCD (PQCD) method, where P represents a pseudoscalar meson, and V refers to ρ, ω, and ϕ mesons. We present the amplitude of the quasi-two-body decay process and investigate the effects of mixed resonances involving $\rho^0-\omega$, $\rho^0-\phi$, and $\omega-\phi$ while considering the impact of isospin symmetry breaking. We observe significant CP asymmetry when the invariant mass of the $\pi^+\pi^-$ pair is within the resonance ranges of ρ, ω, and ϕ mesons. Consequently, we quantify the regional CP asymmetry in these resonance regions. A significant difference is observed when comparing the results obtained with and without the interference of the three vector mesons and isospin conservation. The CP asymmetry results obtained from the three-body decay process, without interference owing to isospin conservation by the PQCD method, are in agreement with the newly updated data acquired by the LHCb experiment.

Keywords: CP asymmetry, B meson decay, heavy flavor physics

DOI: 10.1088/1674-1137/adb2f7 **CSTR:** 32044.14.ChinesePhysicsC.49053106

I. INTRODUCTION

CP asymmetry, which plays a crucial role in elucidating the matter-antimatter asymmetry of the universe, holds significant theoretical and experimental importance in the field of particle physics [1, 2]. CP asymmetry has been experimentally observed in the decay processes of K, B, and D mesons [3−5]. CP asymmetry is closely related to weak and strong phases. The CKM matrix describes the mixing between different quark flavors and carries the phase information responsible for CP asymmetry. The weak phase originates from the CKM matrix, which represents the transformation of quarks from their mass eigenstates to weak interaction eigenstates. Meanwhile, the strong phase arises from hadronic matrices and intermediate states [6]. Recently, CP asymmetry has been observed in the course of B-meson multi-body decays in experiments [7, 8]. The investigation of CP asymmetry in multi-body decays of B mesons plays an increasingly pivotal role in both scrutinizing the CKM mechanism of the SM and exploring novel sources of CP asymmetry [9].

In contrast to the two-body decay, the three-body decay of B meson encompasses both resonance and non-resonance contributions, in addition to being influenced by final state re-scattering in $KK\to\pi\pi$ interactions [10]. The observation of significant CP asymmetry in localized regions of phase space for charmless three-body B-meson decays has been reported through model-independent analyses. In LHCb experiments, researchers have conducted extensive investigations into the full phase space of B meson decays, with particular emphasis on a specific invariant mass region. The CP asymmetry in the $B^\pm\to\pi^+\pi^-\pi^\pm$ decay process is denoted as $A_{CP}^{\rm inte}$ across the entire phase space, with a measured value of $A_{CP}^{\rm inte}=(5.8\pm0.8\pm0.9\pm0.7)\%$. In the specified invariant mass regions, for the low invariant mass region in which $m^2_{\pi^+\pi^-\ {\rm low}}<0.4\ {\rm GeV}^2$ and the high invariant mass region in which $m^2_{\pi^+\pi^-\ {\rm high}}<15\ {\rm GeV}^2$, the CP asymmetry is represented by $A_{CP}^{\rm low}$, with a corresponding value of $A_{CP}^{\rm low}=(58.4\pm8.2\pm2.7\pm0.7)\%$. In the rescattering region, defined by $m^2_{\pi^+\pi^-\ {\rm high}}<15\ {\rm GeV}^2$, the CP asymmetry is denoted as $A_{CP}^{\rm resc}$, with a measured value of $A_{CP}^{\rm resc}=(17.2\pm2.1\pm1.2\pm0.7)\%$ [11,

Received 2 November 2024; Accepted 27 January 2025; Published online 28 January 2025
* Supported by the Natural Science Foundation of Henan Province, China(252300420319) and the National Natural Science Foundation of China (12275024)
† E-mail: 1904132420@qq.com
‡ E-mail: ganglv66@sina.com
§ E-mail: xhguo@bnu.edu.cn
♮ E-mail: ouhaifeng@haut.edu.cn

12]. The data were extracted from the $B^{\pm} \to \pi^+\pi^-K^{\pm}$ decay to measure the integrated CP asymmetry over the full phase space, where $A_{CP}^{\rm inte}$ is determined as $(2.5 \pm 0.4 \pm 0.4 \pm 0.7)\%$. Furthermore, measurements were conducted in specific regions: the low invariant mass region ($0.08\,{\rm GeV}^2 < m^2_{\pi^+\pi^-} < 0.66\,{\rm GeV}^2$) and the high invariant mass region ($m^2_{\pi^{\pm}K^{\pm}} > 15\,{\rm GeV}^2$), yielding $A_{CP}^{\rm low}$ values of $(67.8 \pm 7.8 \pm 3.2 \pm 0.7)\%$ and $A_{CP}^{\rm resc}$ values of $(12.1 \pm 1.2 \pm 1.7 \pm 0.7)\%$ in the rescattering regions with $1.0\,{\rm GeV} < m_{\pi^+\pi^-} < 1.5\,{\rm GeV}$ [10, 12].

The three-body decay process contains intricate dynamical information. In the LHCb experiment, the decay of three-body B mesons is analyzed using the Dalitz plot [10, 12]. The characteristics of the resonance amplitudes can be clearly observed from the Dalitz diagram, revealing that scalar and vector resonances with invariant masses of less than approximately 1 GeV/c^2 are dominant [13]. In the decay of charged B meson, the Dalitz diagram shows that evident CP asymmetry exists when the invariant masses of $\pi^+\pi^-$ are in the $\rho^0(770)$ and $f_0(980)$ resonance regions [14, 15]. Until recently, a resonance model that accurately describes these effects has been lacking [7, 8]. Our previous results showed that there is a large CP asymmetry at the regions of the $\rho^0(770)$ and $\omega(782)$ resonance for B meson decay process [16−20].

The three-body charmless decay of B mesons is primarily governed by a quasi-two-body process involving an intermediate resonance state. The effects of this resonance can be accurately described using the Breit-Wigner (BW) formalism. To achieve a comprehensive understanding of CP asymmetry, various theoretical frameworks have been employed to describe the multibody decays of B mesons, including QCD factorization (QCDF) [16, 17] and perturbative QCD (PQCD) [18, 21]. In the decay process of the B meson, different methods introduce different phases, thereby affecting the value of CP asymmetry. In the QCDF method, the b-quark mass m_b is considered to approach infinity in the decay of the B meson, while neglecting the higher-order contribution of $1/m_b$. The consideration is solely focused on the longitudinal momentum, while the transverse momentum, which is relatively small in magnitude, can be disregarded when compared to its longitudinal counterpart [22]. The PQCD approach preserves the k_T transverse momentum, selects an appropriate scale, and introduces Sudakov factors to resolve endpoint divergences [23, 24]. Our objective is to investigate the CP asymmetry associated with vector meson resonances in the three-body decay of B mesons using the PQCD method.

According to the Vector Meson Dominated (VMD) model, the polarization of photons in vacuum leads to the emergence of vector particles such as ρ^0, ω, and ϕ. The annihilation of e^+e^- into photons results in the production of a pair of $\pi^+\pi^-$ through an intermediate neutral vector meson. The decay of ρ^0 into $\pi^+\pi^-$ is an isospin-conserving process, while the decays of ω and ϕ into $\pi^+\pi^-$ involve isospin asymmetry. To better describe these decay processes, we utilize a unitary matrix transformation to convert the isospin of the intermediate state (non-physical states) into a physical field. By observing interference between the resonant mesons (ρ^0, ω, and ϕ), valuable insights into their kinetic mechanisms can be obtained. Furthermore, it should be noted that the presence of intermediate resonance hadrons contributes to the formation of a new strong phase, which may have implications for CP asymmetry in hadronic decays. We investigate the impact of mixed resonance of intermediate particles on CP asymmetry in the three-body decay process of B meson. Examining the decay of vector meson resonances will enable more precise measurement of CP asymmetry in future experiments. In addition, we discuss regional variations in CP asymmetry for comparison with experimental results.

The layout of the present paper is as follows: In Sec. II, we discuss resonant contributions to three-body decays of B mesons. The quasi-two-body method $B \to VP(V \to PP)$ is employed to investigate the CP asymmetry. Sec. III is dedicated to the examination of direct CP asymmetry. The regional CP asymmetries arising from the resonance effects of ρ^0, ω, and ϕ are considered. We illustrate the form of the three-body decay amplitude of the B meson after considering the above resonance effect and present the CP asymmetry. The numerical results of and a discussion on the local CP asymmetry are presented in Sec. IV. Sec. V presents our conclusions.

II. EFFECT OF VECTOR MESON RESONANCE ON THREE-BODY DECAY OF *B* MESON

A. Mixing mechanism

Based on the VMD model, electrons and positrons annihilate to generate photons, which are further polarized to form vector mesons ρ^0, ω, and ϕ. Then, these vector mesons decay into a pair of $\pi^+\pi^-$ mesons [19]. In this mechanism, the mixing parameters corresponding to two vector particles can be obtained by using the electromagnetic form factor of the π meson.

As the ρ_I^0 (ω_I, ϕ_I) resonance state is a non-physical state, we use the unitary matrix R to transform the isospin field into the physical field: $\rho_I^0(\omega_I,\phi_I) \to \rho^0(\omega,\phi)$. The diagonal elements of the unitary matrix R are equal to 1, while the off-diagonal elements encode information regarding the $\rho^0-\omega-\phi$ mixture. The contribution of high order terms is ignored in the process of this transformation. The resonance effects for $A_{\rho\omega}, B_{\omega\phi}$, and $C_{\rho\phi}$ are defined by a set of mixed amplitude parameters, where it holds that $A_{\rho^0\omega} = -A_{\omega\rho^0}$, $B_{\omega\phi} = -B_{\phi\omega}$, and $C_{\rho^0\phi} = -C_{\phi\rho^0}$. The amplitude represents a first-order approximation that is dependent on the variable s, which in turn is related to the square of momentum. The expression is

$$\begin{pmatrix} \rho^0 \\ \omega \\ \phi \end{pmatrix} = R(s) \begin{pmatrix} \rho_I^0 \\ \omega_I \\ \phi_I \end{pmatrix} = \begin{pmatrix} 1 & -A_{\rho\omega}(s) & -C_{\rho\phi}(s) \\ A_{\rho\omega}(s) & 1 & -B_{\omega\phi}(s) \\ C_{\rho\phi}(s) & B_{\omega\phi}(s) & 1 \end{pmatrix} \begin{pmatrix} \rho_I^0 \\ \omega_I \\ \phi_I. \end{pmatrix}. \tag{1}$$

According to the transformation relation of the R matrix, the expression form of the resonance state in the physical state is given as $\phi = C_{\rho^0\phi}(s)\rho_I^0 + B_{\omega\phi}(s)\omega_I + \phi_I$, $\omega = A_{\rho^0\omega}(s)\rho_I^0 + \omega_I - B_{\omega\phi}(s)\phi_I$, $\rho^0 = \rho_I^0 - A_{\rho^0\omega}(s)\omega_I - C_{\rho^0\phi}(s)\phi_I$ [20].

We define the mixing parameters $\Pi_{V_iV_j}$ (where V_i and V_j represent distinct vector mesons) as [18, 25]

$$\begin{aligned} A_{\rho^0\omega} = -A_{\omega\rho^0} &= \frac{\Pi_{\rho^0\omega}}{(s - m_{\rho^0}^2 + \mathrm{i}m_{\rho^0}\Gamma_{\rho^0}) - (s - m_\omega^2 + \mathrm{i}m_\omega\Gamma_\omega)}, \\ B_{\omega\phi} = -B_{\phi\omega} &= \frac{\Pi_{\omega\phi}}{(s - m_\omega^2 + \mathrm{i}m_\omega\Gamma_\omega) - (s - m_\phi^2 + \mathrm{i}m_\phi\Gamma_\phi)}, \\ C_{\rho^0\phi} = -C_{\phi\rho^0} &= \frac{\Pi_{\rho^0\phi}}{(s - m_{\rho^0}^2 + \mathrm{i}m_{\rho^0}\Gamma_{\rho^0}) - (s - m_\phi^2 + \mathrm{i}m_\phi\Gamma_\phi)}. \end{aligned} \tag{2}$$

The term $s - m_v^2 + \mathrm{i}m_v\Gamma_v$ represents the inverse of the vector meson propagator, where s denotes the invariant mass squared of the $\pi^+\pi^-$ meson [26]. The decay width of the vector meson is indicated by Γ_V, and the mass of the vector meson is represented by m_V.

The parameters $A_{\rho^0\omega}$, $B_{\omega\phi}$, $C_{\rho^0\phi}$, and $\Pi_{V_iV_j}$ are considered as first-order approximations. Any product of two parameters can be disregarded owing to its higher-order nature. We hereby define

$$\begin{aligned} \widetilde{\Pi}_{\rho^0\omega} &= \frac{(s - m_{\rho^0}^2 + \mathrm{i}m_{\rho^0}\Gamma_{\rho^0})\Pi_{\rho^0\omega}}{(s - m_{\rho^0}^2 + \mathrm{i}m_{\rho^0}\Gamma_{\rho^0}) - (s - m_\omega^2 + \mathrm{i}m_\omega\Gamma_\omega)}, \\ \widetilde{\Pi}_{\rho^0\phi} &= \frac{(s - m_{\rho^0}^2 + \mathrm{i}m_{\rho^0}\Gamma_{\rho^0})\Pi_{\rho^0\phi}}{(s - m_{\rho^0}^2 + \mathrm{i}m_{\rho^0}\Gamma_{\rho^0}) - (s - m_\phi^2 + \mathrm{i}m_\phi\Gamma_\phi)}, \\ \widetilde{\Pi}_{\omega\phi} &= \frac{(s - m_\phi^2 + \mathrm{i}m_\phi\Gamma_\phi)\Pi_{\omega\phi}}{(s - m_\omega^2 + \mathrm{i}m_\omega\Gamma_\omega) - (s - m_\phi^2 + \mathrm{i}m_\phi\Gamma_\phi)}. \end{aligned} \tag{3}$$

Through the derivation process of the mixed parameters, it can be inferred that a correlation exists between the mixed parameters and s. These mixed parameters amalgamate the contributions from both resonant and non-resonant components arising owing to isospin symmetry breaking effects in the direct decay process, while also exhibiting momentum dependence. Based on the available experimental results, we can accurately determine the mixing parameters $\Pi_{\rho^0\omega} = -4470 \pm 250 \pm 160 - \mathrm{i}(5800 \pm 2000 \pm 1100)\ \mathrm{MeV}^2$ in the vicinity of the ρ^0 meson. The mixing parameters $\Pi_{\phi\rho^0} = 720 \pm 180 - \mathrm{i}(870 \pm 320)\ \mathrm{MeV}^2$ are obtained near the ϕ meson [27, 28]. Isospin symmetry is manifested in the decay of the B meson as the ρ meson decay to $\pi^+\pi^-$ satisfies isospin conservation, while the decay of ω and ϕ mesons violates this conservation.

B. CP asymmetry induced by interference

The decay $B \to (V \to \pi^+\pi^-)\pi(K)$ is modeled as a quasi-two-body process, where V represents an intermediate vector meson. The presence of vector meson resonances in the decay process significantly impacts the strong phase, tree, and penguin amplitudes. In Fig. 1, for the decay of $B \to [\rho^0(\omega,\phi) \to \pi^+\pi^-]\pi(K)$, we investigate the impacts of various vector meson resonances.

According to the three-vector meson mixing mechanism, and neglecting the contribution of higher order terms, we can derive the decay diagram for the $B \to [\rho^0(\omega,\phi) \to \pi^+\pi^-]\pi(K)$ decay process, as illustrated in diagrams $(a) \sim (i)$ of Fig. 1. In diagram (a), it can be observed that the B meson directly decays to produce a pair of $\pi^+\pi^-$ mesons through the intermediate state of the ρ^0 meson. Simultaneously, it is evident that both the ω and ϕ mesons also contribute to the production of a pair of $\pi^+\pi^-$ mesons through direct decays: $\phi \to \pi\pi$ and $\omega \to \pi\pi$, as shown in diagrams (d) and (g), respectively.

We illustrate various effects arising from mixed resonances in diagrams (b), (c), (e), (f), (h), and (i) of Fig. 1. In addition to the direct decay of vector mesons (ρ^0, ω, and ϕ) into a pair of $\pi^+\pi^-$ mesons, the production of such meson pairs can also occur through resonances of vector mesons. During this decay process, isospin symmetry is violated. The black dots in the diagram represent mixing, expressed as $\Pi_{\mathrm{V_iV_j}}$. As shown in diagrams (e) and (h), the ϕ and ω mesons respectively resonate with the ρ^0 meson, and subsequently, the ρ^0 meson decays further into a pair of $\pi^+\pi^-$ mesons. The corresponding mixing parameters are $\Pi_{\rho^0\phi}$ and $\Pi_{\rho^0\omega}$, where $\Pi_{\rho^0\phi}$ is generated in the $\phi - \rho^0$ resonance process and $\Pi_{\rho^0\omega}$ is generated in the $\omega - \rho^0$ resonance process. Diagrams (b) and (c) illustrate the decay processes of the ρ^0 meson into a pair of $\pi^+\pi^-$ mesons via ϕ and ω resonances, respectively.

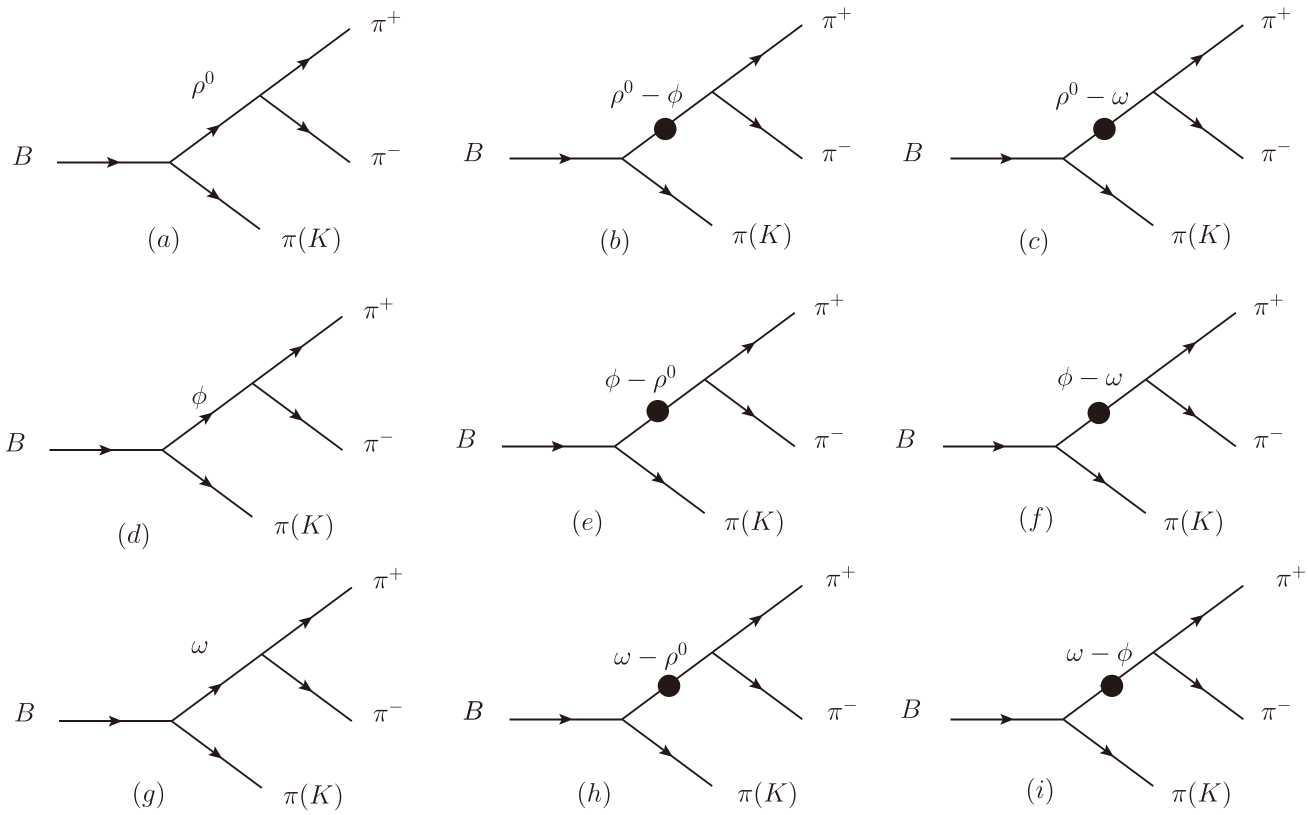

Fig. 1. Diagrams of $B\to\pi^+\pi^-\pi(K)$ decay process.

The decay of the ω and ϕ mesons into a pair of $\pi^+\pi^-$ mesons violates the law of isospin conservation. However, considering the small mixing parameter, the contribution arising from the mixing of ω and ϕ can be treated as a higher-order term that may be neglected. Consequently, we can disregard the contributions from diagrams (b), (c), (f), and (i). An amplitude analysis of this decay channel reveals that ρ^0 dominates the contribution [29–31]. However, it is crucial to consider the strong phase generated by the mixed resonance and its impact on CP asymmetry. It should be noted that the mixed parameters $\Pi_{\rho^0\phi}$ and $\Pi_{\rho^0\omega}$ are approximations at the first order.

The amplitudes for diagrams (a), (e), and (h) in Fig. 1 are represented by A_a, A_e, and A_h, respectively. We provide the amplitude expression for the three-body decay process $B\to\pi^+\pi^-\pi(K)$ as follows:

$$A = A_a + A_e + A_h. \tag{4}$$

According to Fig. 1, the quasi-two-body approach is adopted to compute the CP asymmetry in B meson decays. The symbol $\mathcal{A}(\rho^0\pi)$ denotes the decay amplitudes of the $B\to\rho^0\pi$ process. The term $s-m_{\rho^0}^2+\mathrm{i}m_{\rho^0}\Gamma_{\rho^0}$ represents the inverse of the ρ^0 meson propagator. The coupling constant for the $\rho\to\pi\pi$ transition is denoted by $g^{\rho^0\to\pi^+\pi^-}$, with its absolute value denoted by $|g^{\rho(770)\to\pi^+\pi^-}| = 6.00$ [32, 33]. The coupling constant is a complex number, as reported in reference [33]. The strong phase has been incorporated into the mixing parameter, which was determined through experimental fitting. In diagram (a), the amplitude expression for the direct decay of the ρ^0 meson is presented as follows:

$$A_a = \frac{g^{\rho^0\to\pi^+\pi^-}}{s-m_{\rho^0}^2+\mathrm{i}m_{\rho^0}\Gamma_{\rho^0}}\mathcal{A}(\rho^0\pi). \tag{5}$$

Based on the contributions depicted in diagrams (e) and (h) within the framework of the PQCD approach, we have derived the decay amplitudes A_e and A_h that encompass mixed contributions, expressed as follows:

$$A_e = \frac{g^{\rho^0\to\pi^+\pi^-}}{(s-m_{\rho^0}^2+\mathrm{i}m_{\rho^0}\Gamma_{\rho^0})(s-m_{\phi}^2+\mathrm{i}m_{\phi}\Gamma_{\phi})}\widetilde{\Pi}_{\rho^0\phi}\mathcal{A}(\phi\pi), \tag{6}$$

$$A_h = \frac{g^{\rho^0\to\pi^+\pi^-}}{(s-m_{\rho^0}^2+\mathrm{i}m_{\rho^0}\Gamma_{\rho^0})(s-m_{\omega}^2+\mathrm{i}m_{\omega}\Gamma_{\omega})}\widetilde{\Pi}_{\rho^0\omega}\mathcal{A}(\omega\pi), \tag{7}$$

where $\mathcal{A}(\phi\pi)$ and $\mathcal{A}(\omega\pi)$ represent the decay amplitudes of $B\to\phi\pi$ and $B\to\omega\pi$, respectively. We define the differential parameter of CP asymmetry as

$$A_{\rm CP}=\frac{|A|^2-|\overline{A}|^2}{|A|^2+|\overline{A}|^2}. \tag{8}$$

C. Regional CP asymmetry

Recently, the LHCb experiment yielded significant discoveries by directly measuring CP asymmetry in charmless decays of B mesons involving three-body final states, providing evidence for substantial values within a specific region of the phase space. The decay process $B_u^-\to\pi^+\pi^-\pi^-$ exhibits a significant CP asymmetry within the invariant mass region ($m^2_{\pi^+\pi^-\,\rm low}<0.4\,{\rm GeV}^2$) [12]. In this study, we compute the $A_{\rm CP}$ integrals to facilitate comparison with experimental observations.

The amplitude of the $B_u^-\to\rho^0\pi^-$ decay can be expressed as $M^\lambda_{B_u^-\to\rho^0\pi^-}=\alpha P_{B_u^-}\cdot\epsilon^*(\lambda)$, where α represents the contribution from PQCD and is independent of the polarization state λ. Here, $P_{B_u^-}$ denotes the momentum of the B_u^- meson, ϵ is the polarization vector of the ρ^0 meson, and λ specifies the polarization direction of ϵ. The amplitude for the $\rho^0\to\pi^+\pi^-$ decay can be written as $M^\lambda_{\rho^0\to\pi^+\pi^-}=g^{\rho^0\to\pi^+\pi^-}\epsilon(\lambda)\cdot\left(p_\pi^+-p_\pi^-\right)$, where $g^{\rho^0\to\pi^+\pi^-}$ is the effective coupling constant, and ϵ represents the polarization vector of the ρ^0 meson. Hence, the amplitude of $B_u^-\to\rho^0(\rho^0\to\pi^+\pi^-)\pi^-$ is

$$\begin{aligned}A&=\frac{g^{\rho^0\to\pi^+\pi^-}\alpha}{(s-m^2_{\rho^0}+{\rm i}m_{\rho^0}\Gamma_{\rho^0})}P^\mu_{B_u^-}\sum_{\lambda=\pm1,0}\epsilon^*_\mu(\lambda)\epsilon_r(\lambda)\cdot\left(p_\pi^+-p_\pi^-\right)^r\\&=-\frac{g^{\rho^0\to\pi^+\pi^-}\alpha}{(s-m^2_{\rho^0}+{\rm i}m_{\rho^0}\Gamma_{\rho^0})}P^\mu_{B_u^-}\left[g_{\mu r}-\frac{\left(p_\pi^++p_\pi^-\right)_\mu\left(p_\pi^++p_\pi^-\right)_r}{m^2_{\rho^0}}\right]\left(p_\pi^+-p_\pi^-\right)^r=\frac{g^{\rho^0\to\pi^+\pi^-}}{(s-m^2_{\rho^0}+{\rm i}m_{\rho^0}\Gamma_{\rho^0})}\cdot\frac{M^\lambda_{B_u^-\to\rho^0\pi^-}}{p_{B_u^-}\cdot\epsilon^*}\cdot(\Sigma-s').\end{aligned} \tag{9}$$

In the three-body decay process, we utilize the principles of momentum and energy conservation to transform the equation as follows: $P_{B_u^-}=p_\pi^++p_\pi^-+p_\pi^-$ and $m^2_{ij}=p^2_{ij}$, aiming to facilitate computational procedures. Here, $\sqrt{s}$ and $\sqrt{s'}$ represent the low and high invariant masses of the pair of $\pi^+\pi^-$ mesons, respectively. By fixing the variable s and considering the dependency between its values, we can determine an appropriate value s' that satisfies the formula $\Sigma=1/2\left(s'_{\rm max}+s'_{\rm min}\right)$, where $s'_{\rm max}$ and $s'_{\rm min}$ represent the maximum and minimum values, respectively [14]. According to the kinetic principles of the three-body decay process, we can derive the regional CP asymmetry in the $B_u^-\to\pi^+\pi^-\pi^-$ decay process within a certain invariant mass range:

$$A^\Omega_{\rm CP}=\frac{\int_{s_1}^{s_2}{\rm d}s\int_{s'_1}^{s'_2}{\rm d}s'\left(\Sigma-s'\right)^2\left(|A|^2-|\overline{A}|^2\right)}{\int_{s_1}^{s_2}{\rm d}s\int_{s'_1}^{s'_2}{\rm d}s'\left(\Sigma-s'\right)^2\left(|A|^2+|\overline{A}|^2\right)}. \tag{10}$$

The numerator and denominator of $A_{\rm CP}$ can be integrated over the range $\Omega\left(s_1<s<s_2, s'_1<s'<s'_2\right)$. The integration interval for the high-invariant mass of the $\pi^+\pi^-$ meson pair is $s'_1<s'<s'_2$, where $\int_{s'_1}^{s'_2}{\rm d}s'(\Sigma-s')^2$ represents a factor dependent on s'. Through kinematic analysis, the correlation between Σ and s' can be readily determined. Assuming a finite range, we can consider Σ to be constant. Consequently, the term $\int_{s'_1}^{s'_2}{\rm d}s'\left(\Sigma-s'\right)^2$ becomes negligible in the calculation, rendering $A^\Omega_{\rm CP}$ independent of the high invariant mass of positive and negative particles. In the $B\to\pi^+\pi^-K$ decay process, a similar method can also be used to calculate regional CP asymmetry.

III. CALCULATION PROCESS AND ANALYSIS OF CP ASYMMETRY

In the calculation of CP asymmetry, we consider the contribution of the mixed resonance mechanism to the three-body decay amplitude. For B meson decays, the PQCD method is employed to separate the decay process into its hard components and non-perturbative parts. The hard components are isolated and analyzed using perturbative theory, while the non-perturbative parts are incorporated into universal meson wave functions. The decay of B mesons involves intricate dynamical phenomena, wherein a light quark exhibits significant kinetic energy while the spectator quark remains relatively stationary. Subsequently, the spectator quark undergoes an exchange of a high-energy gluon, thereby acquiring additional kinetic energy and accelerating to combine with a light quark, resulting in the production of a rapidly moving final meson. The final meson further decays into the pair of $\pi^+\pi^-$ mesons, and the transverse momentum (k_T) is retained in the PQCD method. To handle endpoint divergences, the Sudakov factor is introduced to suppress long-range interactions in the small transverse momentum range, thereby ensuring that the entire process can be perturbatively calculated effectively [34, 35]. The parameters used in the calculation are derived from Table 1.

Table 1. Other parameters are from [24, 33, 36].

Mass (GeV)	m_{B_u} = 5279.34±0.12	m_{B_d} = 5.27965±0.12	$m_{\pi^\pm}$ = 139.57	m_{π^0} = 134.98
	m_{K^0} = 497.611±0.013	m_ρ = 775.26±0.25	m_ω = 782.65±0.12	m_ϕ = 1019.461±0.016
Wolfenstein parameters	$\lambda = 0.22650\pm0.00048$	$A = 0.790^{+0.017}_{-0.012}$	$\bar{\rho} = 0.141^{+0.016}_{-0.017}$	$\bar{\eta} = 0.357\pm0.011$
Decay constants (GeV)	f_B = 190.0±1.3	f_π = 130.2±1.2	f_K = 155.7±0.3	$f^T_\phi = 0.22$
	$f_\omega = 0.195$	$f_\phi = 0.23$	$f_\rho = 0.209$	$f^T_\omega = 0.14$
Decay width (GeV)	$\Gamma_\rho = 0.15$	$\Gamma_\omega = 8.49\times10^{-3}$	$\Gamma_\phi = 4.23\times10^{-3}$	

A. CP asymmetry analysis of the $B^-_u \to (\rho^0,\omega,\phi \to \pi^+\pi^-)\pi^-$ decay process

The Dalitz diagram analysis of the decay amplitude $B^\pm \to \pi^+\pi^-\pi^\pm$ in two-dimensional phase space is performed, as indicated by the relevant literature [11]. Phenomenological investigations have primarily focused on exploring regional CP asymmetries in the decay process $B^\pm \to \pi^+\pi^-\pi^\pm$, with certain studies emphasizing the significance of the $\rho^0-\omega$ mixing effects between ρ^0 and ω, highlighting potential interference between the resonance of ρ^0 and the broad *S*-wave contribution [11, 12]. The resonance contributions of $\rho-\omega$, $\omega-\phi$, and $\rho-\phi$ can give rise to a novel strong phase. To facilitate clearer observation, we select the energy range of 0.7 GeV to 1.1 GeV, which corresponds to the primary region in which significant effects of decay processes involving ρ^0, ω, and ϕ resonances are exhibited.

We can obtain the Dalitz diagram for the *B* meson decay process from experiments. By analyzing the Dalitz diagram, we can determine the existence of resonance states, study the energy momentum relationships in the decay process, and further explore the impact of resonance and non-resonance contributions on the *B* meson three-body decay process. However, because the *B* meson phase space allows for multiple types of resonances to exist, there may be a large number of intermediate states. Investigating these resonance structures is a complex task and it should be noted that it is not possible to distinguish between the contributions made by the ρ^0 meson and ω meson in experiments.

Using the PQCD method and considering the CKM matrix elements $V_{ub}V^*_{ud}$ and $V_{tb}V^*_{td}$ in the $B^-_u \to (\rho^0, \to \pi^+\pi^-)\pi^-$ three-body decay process, we can provide the amplitude expression for CP asymmetry. Fig. 1 encompasses the direct decay modes of the vector meson and the mixed resonance decay modes of two vector mesons. The three-body decay amplitude of the *B* meson in diagram (a) of Fig. 1 is expressed as follows:

$$
\begin{aligned}
A(a) =& A(B^-_u \to (\rho^0 \to \pi^+\pi^-)\pi^-) = \sum_{\lambda=0,\pm1} \frac{G_F P_{B^-_u}\cdot\epsilon^*(\lambda)\; g^{\rho^0\to\pi^+\pi^-}\epsilon(\lambda)\cdot(p_{\pi^+}-p_{\pi^-})}{2(s-m^2_{\rho^0}+\mathrm{i}m_{\rho^0}\Gamma_{\rho^0})} \times \Big\{ V_{ub}V^*_{ud}\big\{a_1\big[\mathcal{A}^{LL}_{ab}(\pi,\rho)\\
&+\mathcal{A}^{LL}_{ef}(\pi,\rho)-\mathcal{A}^{LL}_{ef}(\rho,\pi)\big]+a_2\mathcal{A}^{LL}_{ab}(\rho,\pi)+C_2\big[\mathcal{A}^{LL}_{cd}(\pi,\rho)+\mathcal{A}^{LL}_{gh}(\pi,\rho)-\mathcal{A}^{LL}_{gh}(\rho,\pi)\big]+C_1\mathcal{A}^{LL}_{cd}(\rho,\pi)\big\}\\
&-V_{tb}V^*_{td}\Big\{(a_4+a_{10})\big[\mathcal{A}^{LL}_{ab}(\pi,\rho)+\mathcal{A}^{LL}_{ef}(\pi,\rho)-\mathcal{A}^{LL}_{ef}(\rho,\pi)\big]+(a_6+a_8)\big[\mathcal{A}^{SP}_{ab}(\pi,\rho)+\mathcal{A}^{SP}_{ef}(\pi,\rho)-\mathcal{A}^{SP}_{ef}(\rho,\pi)\big]\\
&-\left(a_4-\frac{3}{2}a_7-\frac{3}{2}a_9-\frac{1}{2}a_{10}\right)\mathcal{A}^{LL}_{ab}(\rho,\pi)+(C_3+C_9)\big[\mathcal{A}^{LL}_{cd}(\pi,\rho)+\mathcal{A}^{LL}_{gh}(\pi,\rho)-\mathcal{A}^{LL}_{gh}(\rho,\pi)\big]+(C_5+C_7)\big[\mathcal{A}^{SP}_{cd}(\pi,\rho)\\
&+\mathcal{A}^{SP}_{gh}(\pi,\rho)-\mathcal{A}^{SP}_{gh}(\rho,\pi)\big]-\left(C_3-\frac{3}{2}C_{10}-\frac{1}{2}C_9\right)\mathcal{A}^{LL}_{cd}(\rho,\pi)+\frac{3}{2}C_8\mathcal{A}^{LR}_{cd}(\rho,\pi)-\left(C_5-\frac{1}{2}C_7\right)\mathcal{A}^{SP}_{cd}(\rho,\pi)\Big\}\Big\}.
\end{aligned}
\tag{11}
$$

The momentum parameter P_i ($P_i = P_{B^-_u}$, p_{π^+}, p_{π^-}) is defined, where ϵ represents the polarization vector of the vector meson. The Fermi coupling constant is denoted as G_F. C_i is the Wilson coefficient, and a_i is related to the Wilson coefficient C_i [37]. Three flow structures are labeled as LL, LR, and SP. $\mathcal{A}_{ab}$ refers to the contribution of factorizable emission diagrams, whereas $\mathcal{A}_{cd}$ represents the contribution of nonfactorizable emission diagrams. Similarly, $\mathcal{A}_{ef}$ ($\mathcal{A}_{gh}$) denotes the contribution of factorizable (nonfactorizable) annihilation diagrams. $V_{ub}V^*_{ud}$ and $V_{tb}V^*_{td}$ can be measured experimentally and theoretically represented by the Wolfstein parameters A, ρ, λ, and η: $V_{ub}V^*_{ud} = A\lambda^3(\rho-\mathrm{i}\eta)\left(1-\frac{\lambda^2}{2}\right)$ and $V_{tb}V^*_{td} = A\lambda^3(1-\rho+\mathrm{i}\eta)$.

Diagrams (d) and (g) of Fig. 1 represent the direct decay process of the ϕ and ω mesons, respectively, producing the pair of $\pi^+\pi^-$ mesons. Owing to isospin symmetry breaking, the contributions of ω and ϕ to this decay can be neglected. The specific expression of the three-body decay amplitude in the vector meson resonance, as shown in diagram (e), is as follows:

$$A(e) = A(B_u^- \to (\phi - \rho^0 \to \pi^+\pi^-)\pi^-) = \sum_{\lambda=0,\pm1} \frac{-G_F P_{B_u^-} \cdot \epsilon^*(\lambda)\ g^{\rho^0\to\pi^+\pi^-} \epsilon(\lambda)\cdot(p_{\pi^+} - p_{\pi^-})}{2(s - m_{\rho^0}^2 + \mathrm{i} m_{\rho^0}\Gamma_{\rho^0})(s - m_\phi^2 + \mathrm{i} m_\phi \Gamma_\phi)} \tilde{\Pi}_{\rho^0\phi}$$
$$\times \left\{ V_{tb} V_{td}^* \left\{ \left(a_3 + a_5 - \frac{1}{2}a_7 - \frac{1}{2}a_9\right) \mathcal{A}_{ab}^{LL}(\phi,\pi) + \left(C_4 - \frac{1}{2}C_{10}\right) \mathcal{A}_{cd}^{LL}(\phi,\pi) + (C_6 - \frac{1}{2}C_8)\mathcal{A}_{cd}^{LR}(\phi,\pi)\right\}\right\}. \tag{12}$$

The ω meson and ρ^0 meson undergo resonance, and subsequently, the ρ^0 meson decays into the pair of $\pi^+\pi^-$ mesons. The amplitude of the three-body decay shown in diagram (h) of Fig. 1 is as follows:

$$A(h) = A(B_u^- \to (\omega - \rho^0 \to \pi^+\pi^-)\pi^-) = \sum_{\lambda=0,\pm1} \frac{G_F P_{B_u^-} \cdot \epsilon^*(\lambda)\ g^{\rho^0\to\pi^+\pi^-} \epsilon(\lambda)\cdot(p_{\pi^+} - p_{\pi^-})}{2(s - m_{\rho^0}^2 + \mathrm{i} m_{\rho^0}\Gamma_{\rho^0})(s - m_\omega^2 + \mathrm{i} m_\omega \Gamma_\omega)} \tilde{\Pi}_{\rho^0\omega} \left\{ V_{ub} V_{ud}^* \left\{ a_1 \left[\mathcal{A}_{ab}^{LL}(\pi,\omega)\right.\right.\right.$$
$$\left. + \mathcal{A}_{ef}^{LL}(\pi,\omega) + \mathcal{A}_{ef}^{LL}(\omega,\pi)\right] + a_2 \mathcal{A}_{ab}^{LL}(\omega,\pi) + C_2\left[\mathcal{A}_{cd}^{LL}(\pi,\omega) + \mathcal{A}_{gh}^{LL}(\pi,\omega) + \mathcal{A}_{gh}^{LL}(\omega,\pi)\right] + C_1 \mathcal{A}_{cd}^{LL}(\omega,\pi)\right\}$$
$$- V_{tb} V_{td}^* \left\{ (a_4 + a_{10})\left[\mathcal{A}_{ab}^{LL}(\pi,\omega) + \mathcal{A}_{ef}^{LL}(\pi,\omega) + \mathcal{A}_{ef}^{LL}(\omega,\pi)\right] + (a_6 + a_8)\left[\mathcal{A}_{ab}^{SP}(\pi,\omega) + \mathcal{A}_{ef}^{SP}(\pi,\omega) + \mathcal{A}_{ef}^{SP}(\omega,\pi)\right]\right.$$
$$+ \left(2a_3 + a_4 + 2a_5 + \frac{1}{2}a_7 + \frac{1}{2}a_9 - \frac{1}{2}a_{10}\right)\mathcal{A}_{ab}^{LL}(\omega,\pi) + (C_3 + C_9)\left[\mathcal{A}_{cd}^{LL}(\pi,\omega) + \mathcal{A}_{gh}^{LL}(\pi,\omega) + \mathcal{A}_{gh}^{LL}(\omega,\pi)\right]$$
$$+ (C_5 + C_7)\left[\mathcal{A}_{cd}^{SP}(\pi,\omega) + \mathcal{A}_{gh}^{SP}(\pi,\omega) + \mathcal{A}_{gh}^{SP}(\omega,\pi)\right] + \left(C_3 + 2C_4 - \frac{1}{2}C_9 + \frac{1}{2}C_{10}\right)\mathcal{A}_{cd}^{LL}(\omega,\pi)$$
$$\left.\left. + \left(2C_6 + \frac{1}{2}C_8\right)\mathcal{A}_{cd}^{LR}(\omega,\pi) + \left(C_5 - \frac{1}{2}C_7\right)\mathcal{A}_{cd}^{SP}(\omega,\pi)\right\}\right\}. \tag{13}$$

The contributions of the mixed resonance modes $\rho^0-\phi$, $\omega-\phi$, $\rho^0-\omega$, and $\phi-\omega$ to the pair of $\pi^+\pi^-$ mesons are comparatively smaller than those of the direct decay processes, namely $\phi\to\pi\pi$ and $\omega\to\pi\pi$. Hence, we do not consider the contributions from diagrams (b), (c), (f), and (i) in Fig. 1.

We present a diagram illustrating the relationship between CP asymmetry and the invariant mass $\sqrt{s}$ in the quasi-two-body decay $B_u^- \to (\rho^0,\omega,\phi\to\pi^+\pi^-)\pi^-$ within the interference range. The results for the $B_u^-\to\pi^+\pi^-\pi^-$ decay process are presented in Figs. 2 and 3. As depicted in Figs. 2 and 3, it is evident that the CP asymmetry of the $B_u^-\to\pi^+\pi^-\pi^-$ channel undergoes a change when the invariant masses of the $\pi^+\pi^-$ pair encompass the resonance range of ω and ϕ, with a maximum CP asymmetry of 94%. The decay process $B_u^-\to\pi^+\pi^-\pi^-$ exhibits a significant variation in CP asymmetry when the invariant masses of the $\pi^+\pi^-$ pair approach 0.76 GeV, reaching a peak value of 94%. This behavior can be attributed to the effect arising from the mixing mechanism between ρ^0 and ω. Consequently, interference effects are expected within the range of 0.7−0.8 GeV, as indicated by Fig. 2, along with small peaks observed in the invariant mass range corresponding to ϕ according to Fig. 3, in

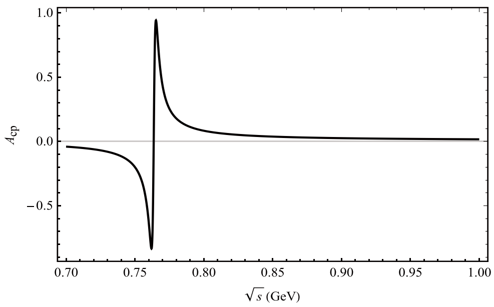

Fig. 2. Plot of A_{CP} as a function of $\sqrt{s}$ corresponding to central parameter values of CKM matrix elements for the decay channel of $B^-\to\pi^+\pi^-\pi^-$.

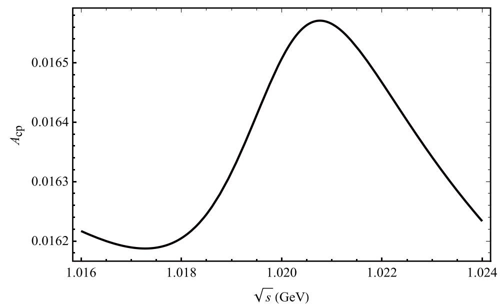

Fig. 3. CP asymmetry plot near the invariant mass of ϕ for the decay channel of $B^-\to\pi^+\pi^-\pi^-$ from the central parameter values of CKM matrix elements.

which the CP asymmetry is measured as 1.6%.

B. CP asymmetry analysis of the $B_u^- \to (\rho^0,\omega,\phi \to \pi^+\pi^-)K^-$ decay process

Experimental observations have revealed that specific regional CP asymmetries in phase space exhibit a greater magnitude compared with the overall CP asymmetry in phase space [13]. The CP asymmetry in the $B^- \to \pi^+\pi^- K^-$ decay process has been measured as $(2.5\pm0.4\pm0.4\pm0.7)\%$ in the full phase space and $(67.8\pm7.8\pm3.2\pm0.7)\%$ within a specified low invariant mass region [10, 12].

Considering the resonance effect of the vector mesons, namely ρ^0, ω, and ϕ, we present the amplitude of the decay process $B_u^- \to (\rho^0,\omega,\phi \to \pi^+\pi^-)K^-$ following a similar mechanism. The three-body direct decay amplitude in diagram (a) of Fig. 1 is as follows:

$$\begin{aligned} A(a) =& A\left(B_u^- \to \left(\rho^0 \to \pi^+\pi^-\right) K^-\right) = \sum_{\lambda=0,\pm1} \frac{G_F P_{B_u^-}\cdot \epsilon^*(\lambda)\ g^{\rho^0\to\pi^+\pi^-}\epsilon(\lambda)\cdot(p_{\pi^+}-p_{\pi^-})}{2(s-m_{\rho^0}^2+\mathrm{i}m_{\rho^0}\Gamma_{\rho^0})} \\ & \times\Big\{V_{ub}V_{us}^*\big\{a_1\left[\mathcal{A}_{ab}^{LL}(K,\rho)+\mathcal{A}_{ef}^{LL}(K,\rho)\right]+a_2\mathcal{A}_{ab}^{LL}(\rho,K)+C_2\left[\mathcal{A}_{cd}^{LL}(K,\rho)+\mathcal{A}_{gh}^{LL}(K,\rho)\right]+C_1\mathcal{A}_{cd}^{LL}(\rho,K)\big\} \\ & -V_{tb}V_{ts}^*\Big\{(a_4+a_{10})\left[\mathcal{A}_{ab}^{LL}(K,\rho)+\mathcal{A}_{ef}^{LL}(K,\rho)\right]+(a_6+a_8)\left[\mathcal{A}_{ab}^{SP}(K,\rho)+\mathcal{A}_{ef}^{SP}(K,\rho)\right] \\ & +\frac{3}{2}(a_7+a_9)\mathcal{A}_{ab}^{LL}(\rho,K)+(C_3+C_9)\left[\mathcal{A}_{cd}^{LL}(K,\rho)+\mathcal{A}_{gh}^{LL}(K,\rho)\right]+(C_5+C_7)\left[\mathcal{A}_{cd}^{SP}(K,\rho)\right. \\ & \left.+\mathcal{A}_{gh}^{SP}(K,\rho)\right]+\frac{3}{2}C_8\mathcal{A}_{cd}^{LR}(\rho,K)+\frac{3}{2}C_{10}\mathcal{A}_{cd}^{LL}(\rho,K)\Big\}\Big\}. \end{aligned} \tag{14}$$

The ϕ meson enters into a resonance with the ρ^0 meson, and subsequently, the ρ^0 meson decays further into the pair of $\pi^+\pi^-$ mesons. The amplitude of the three-body decay shown in diagram (e) of Fig. 1 is as follows:

$$\begin{aligned} A(e) =& A(B_u^- \to (\phi-\rho^0 \to \pi^+\pi^-)K^-) = \sum_{\lambda=0,\pm1} \frac{G_F P_{B_u^-}\cdot \epsilon^*(\lambda)\ g^{\rho^0\to\pi^+\pi^-}\epsilon(\lambda)\cdot(p_{\pi^+}-p_{\pi^-})}{\sqrt{2}(s-m_{\rho^0}^2+\mathrm{i}m_{\rho^0}\Gamma_{\rho^0})(s-m_\phi^2+\mathrm{i}m_\phi\Gamma_\phi)}\tilde{\Pi}_{\rho^0\phi}\Big\{V_{ub}V_{us}^*\big\{a_1\mathcal{A}_{ef}^{LL}(\phi,K) \\ & +C_2\mathcal{A}_{gh}^{LL}(\phi,K)\big\}-V_{tb}V_{ts}^*\Big\{\left(a_3+a_4+a_5-\frac{1}{2}a_7-\frac{1}{2}a_9-\frac{1}{2}a_{10}\right)\mathcal{A}_{ab}^{LL}(\phi,K)+(a_4+a_{10})\mathcal{A}_{ef}^{LL}(\phi,K) \\ & +(a_6+a_8)\mathcal{A}_{ef}^{SP}(\phi,K)+\left(C_3+C_4-\frac{1}{2}C_9-\frac{1}{2}C_{10}\right)\mathcal{A}_{cd}^{LL}(\phi,K)+\left(C_6-\frac{1}{2}C_8\right)\mathcal{A}_{cd}^{LR}(\phi,K)+\left(C_5-\frac{1}{2}C_7\right)\mathcal{A}_{cd}^{SP}(\phi,K) \\ & +(C_3+C_9)\mathcal{A}_{gh}^{LL}(\phi,K)+(C_5+C_7)\mathcal{A}_{gh}^{SP}(\phi,K)\Big\}. \end{aligned} \tag{15}$$

The ω meson and ρ^0 meson undergo resonance, and subsequently, the ρ^0 meson decays into the pair of $\pi^+\pi^-$ mesons. The amplitude of the three-body decay shown in diagram (h) of Fig. 1 is as follows:

$$\begin{aligned} A(h) =& A(B_u^- \to (\omega-\rho^0 \to \pi^+\pi^-)K^-) = \sum_{\lambda=0,\pm1} \frac{G_F P_{B_u^-}\cdot \epsilon^*(\lambda)\ g^{\rho^0\to\pi^+\pi^-}\epsilon(\lambda)\cdot(p_{\pi^+}-p_{\pi^-})}{2(s-m_{\rho^0}^2+\mathrm{i}m_{\rho^0}\Gamma_{\rho^0})(s-m_\omega^2+\mathrm{i}m_\omega\Gamma_\omega)}\tilde{\Pi}_{\rho\omega}\Big\{V_{ub}V_{us}^*\big\{a_1\left[\mathcal{A}_{ab}^{LL}(K,\omega)\right. \\ & \left.+\mathcal{A}_{ef}^{LL}K,\omega)\right]+a_2\mathcal{A}_{ab}^{LL}(\omega,K)+C_2\left[\mathcal{A}_{cd}^{LL}(K,\omega)+\mathcal{A}_{gh}^{LL}(K,\omega)\right]+C_1\mathcal{A}_{cd}^{LL}(\omega,K)\big\}-V_{tb}V_{ts}^*\Big\{(a_4+a_{10})\left[\mathcal{A}_{ab}^{LL}(K,\omega)\right. \\ & \left.+\mathcal{A}_{ef}^{LL}(K,\omega)\right]+(a_6+a_8)\left[\mathcal{A}_{ab}^{SP}(K,\omega)+\mathcal{A}_{ef}^{SP}(K,\omega)\right]+\left(2a_3+2a_5+\frac{1}{2}a_7+\frac{1}{2}a_9\right)\mathcal{A}_{ab}^{LL}(\omega,K)+(C_3+C_9)\left[\mathcal{A}_{cd}^{LL}(K,\omega)\right. \\ & \left.+\mathcal{A}_{gh}^{LL}(K,\omega)\right]+(C_5+C_7)\left[\mathcal{A}_{cd}^{SP}(K,\omega)+\mathcal{A}_{gh}^{SP}(K,\omega)\right]+\left(2C_6+\frac{1}{2}C_8\right)\mathcal{A}_{cd}^{LR}(\omega,K)+\left(2C_4+\frac{1}{2}C_{10}\right)\mathcal{A}_{cd}^{LL}(\omega,K)\Big\}\Big\}. \end{aligned} \tag{16}$$

In Fig. 4, the observed behavior of the CP asymmetry in the $B_u^- \to \pi^+\pi^- K^-$ decay process provides valuable insights into the dynamics of this decay channel. As we approach the resonance range of ω, a significant change in the CP asymmetry is evident, reaching a peak value of 70%. This suggests that there is a strong influence from the ω resonance on the decay process. However, when we consider the resonance range of ϕ, only slight variations

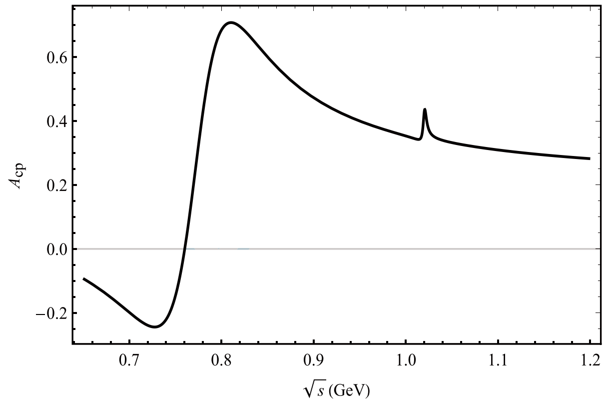

Fig. 4. Plot of $A_{\rm CP}$ as a function of $\sqrt{s}$ corresponding to central parameter values of CKM matrix elements for the decay channel of $B_u^- \to \pi^+\pi^- K^-$.

in CP asymmetry are observed. This can be attributed to several factors. It is worth noting that the specific decay process $B_u^- \to (\phi \to \pi^+\pi^-)K^-$ experiences a further reduction in its overall amplitude owing to interference from $\phi-\rho$ mixing resonance. This interference effect leads to a decrease in observable changes in CP asymmetry within the resonance range of ϕ.

C. CP asymmetry analysis of the $\bar{B}_d^0 \to (\rho^0, \omega, \phi \to \pi^+\pi^-)\pi^0$ decay process

Considering the vector meson ρ^0 - ω - ϕ resonance effect, the process of $\bar{B}_d^0 \to \pi^+\pi^-\pi^0$ can be further elaborated. The presence of these vector mesons in the decay channel introduces additional dynamics and interactions that contribute to the overall behavior of this process. They play a crucial role in understanding strong interactions. In particular, their resonant behavior is associated with a peak in the CP asymmetry for certain energy ranges.

In the decay process of $\bar{B}_d^0 \to \pi^+\pi^-\pi^0$, the vector meson resonance effect refers to how these particles can influence or modify the decay process. By considering this resonance effect, we can gain insights into various aspects of $\bar{B}_d^0 \to \pi^+\pi^-\pi^0$. For instance, it helps us understand how different intermediate states involving vector mesons contribute to the final state particles (pions) observed experimentally. It also provides information regarding possible interference patterns between different amplitudes contributing to this decay process.

The amplitudes of the decay process $\bar{B}_d^0 \to \pi^+\pi^-\pi^0$ arising from various intermediate vector mesons can be presented. The amplitude $\mathcal{A}(\bar{B}_d^0 \to (\rho^0 \to \pi^+\pi^-)\pi^0)$ corresponds to diagram (a) in Fig. 1, which can be expressed as

$$
\begin{aligned}
A(a) =& A(\bar{B}_d^0 \to (\rho^0 \to \pi^+\pi^-)\pi^0) = \sum_{\lambda=0,\pm1} \frac{G_F P_{\bar{B}^0}\cdot\epsilon^*(\lambda)\, g^{\rho^0\to\pi^+\pi^-} \epsilon(\lambda)\cdot(p_{\pi^+}-p_{\pi^-})}{2\sqrt{2}(s-m_{\rho^0}^2+\mathrm{i}m_{\rho^0}\Gamma_{\rho^0})} \Big\{ V_{ub}V_{ud}^* \big\{ a_2 \big[-\mathcal{A}_{ab}^{LL}(\pi,\rho) \\
& -\mathcal{A}_{ab}^{LL}(\rho,\pi) + \mathcal{A}_{ef}^{LL}(\pi,\rho) + \mathcal{A}_{ef}^{LL}(\rho,\pi) \big] + C_1 \big[-\mathcal{A}_{cd}^{LL}(\pi,\rho) - \mathcal{A}_{cd}^{LL}(\rho,\pi) + \mathcal{A}_{gh}^{LL}(\pi,\rho) + \mathcal{A}_{gh}^{LL}(\rho,\pi) \big] \big\} \\
& - V_{tb}V_{td}^* \Big\{ \Big(a_4 - \frac{3}{2}a_9 - \frac{1}{2}a_{10} \Big) \big[\mathcal{A}_{ab}^{LL}(\pi,\rho) + \mathcal{A}_{ab}^{LL}(\rho,\pi) \big] + \frac{3}{2}a_7 \big[\mathcal{A}_{ab}^{LL}(\pi,\rho) - \mathcal{A}_{ab}^{LL}(\rho,\pi) \big] \\
& + \Big(C_3 - \frac{1}{2}C_9 - \frac{3}{2}C_{10} \Big) \big[\mathcal{A}_{cd}^{LL}(\pi,\rho) + \mathcal{A}_{cd}^{LL}(\rho,\pi) \big] - \frac{3}{2}C_8 \big[\mathcal{A}_{cd}^{LR}(\pi,\rho) + \mathcal{A}_{cd}^{LR}(\rho,\pi) \big] + \Big(a_6 - \frac{1}{2}a_8 \Big) \big[\mathcal{A}_{ab}^{SP}(\pi,\rho) \\
& + \mathcal{A}_{ef}^{SP}(\pi,\rho) + \mathcal{A}_{ef}^{SP}(\rho,\pi) \big] + \Big(C_5 - \frac{1}{2}C_7 \Big) \big[\mathcal{A}_{cd}^{SP}(\pi,\rho) + \mathcal{A}_{cd}^{SP}(\rho,\pi) + \mathcal{A}_{gh}^{SP}(\pi,\rho) + \mathcal{A}_{gh}^{SP}(\rho,\pi) \\
& + \Big(2a_3 + a_4 - 2a_5 - \frac{1}{2}a_7 + \frac{1}{2}a_9 - \frac{1}{2}a_{10} \Big) \big[\mathcal{A}_{ef}^{LL}(\pi,\rho) + \mathcal{A}_{ef}^{LL}(\rho,\pi) \big] + \Big(C_3 + 2C_4 - \frac{1}{2}C_9 + \frac{1}{2}C_{10} \Big) \\
& \times \big[\mathcal{A}_{gh}^{LL}(\pi,\rho) + \mathcal{A}_{gh}^{LL}(\rho,\pi) \big] + \Big(2C_6 + \frac{1}{2}C_8 \Big) \big[\mathcal{A}_{gh}^{LR}(\pi,\rho) + \mathcal{A}_{gh}^{LR}(\rho,\pi) \big] \Big\} \Big\},
\end{aligned}
\tag{17}
$$

The vector meson effective mixing resonance modes for the decay process $\bar{B}_d^0 \to (\rho^0 \to \pi^+\pi^-)\pi^0$ are $\phi-\rho^0$ and $\omega-\rho^0$, where the ρ^0 meson undergoes resonance with either the ϕ or ω meson, and subsequently, the ρ^0 meson decays into the pair of $\pi^+\pi^-$ mesons, corresponding to diagrams (e) and (h) of Fig. 1. The three-body decay amplitude forms of the mixing resonance modes are expressed as

$$
\begin{aligned}
A(e) =& A(\bar{B}_d^0 \to (\phi-\rho^0 \to \pi^+\pi^-)\pi^0) = \sum_{\lambda=0,\pm1} \frac{G_F P_{\bar{B}^0}\cdot\epsilon^*(\lambda)\; g^{\rho^0\to\pi^+\pi^-} \epsilon(\lambda)\cdot(p_{\pi^+}-p_{\pi^-})}{2(s-m_{\rho^0}^2+\mathrm{i}m_{\rho^0}\Gamma_{\rho^0})(s-m_\phi^2+\mathrm{i}m_\phi\Gamma_\phi)} \tilde{\Pi}_{\rho^0\phi} \\
& \times \Big\{ V_{tb}V_{td}^* \Big\{ \Big(a_3 + a_5 - \frac{1}{2}a_7 - \frac{1}{2}a_9 \Big) \mathcal{A}_{ab}^{LL}(\phi,\pi) + \Big(C_4 - \frac{1}{2}C_{10} \Big) \mathcal{A}_{cd}^{LL}(\phi,\pi) + \Big(C_6 - \frac{1}{2}C_8 \Big) \mathcal{A}_{cd}^{LR}(\phi,\pi) \Big\} \Big\},
\end{aligned}
\tag{18}
$$

$$A(h)=A(\bar{B}_d^0\to(\omega-\rho^0\to\pi^+\pi^-)\pi^0)=\sum_{\lambda=0,\pm1}\frac{G_F P_{\bar{B}^0}\cdot\epsilon^*(\lambda)\ g^{\rho^0\to\pi^+\pi^-}\epsilon(\lambda)\cdot(p_{\pi^+}-p_{\pi^-})}{2\sqrt{2}(s-m_{\rho^0}^2+\mathrm{i}m_{\rho^0}\Gamma_{\rho^0})(s-m_\omega^2+\mathrm{i}m_\omega\Gamma_\omega)}\tilde{\Pi}_{\rho^0\omega}\Big\{V_{ub}V_{ud}^*\big\{a_2\big[\mathcal{A}_{ab}^{LL}(\pi,\omega)$$
$$-\mathcal{A}_{ab}^{LL}(\omega,\pi)+\mathcal{A}_{ef}^{LL}(\pi,\omega)+\mathcal{A}_{ef}^{LL}(\omega,\pi)\big]+C_1\big[\mathcal{A}_{cd}^{LL}(\pi,\omega)-\mathcal{A}_{cd}^{LL}(\omega,\pi)+\mathcal{A}_{gh}^{LL}(\pi,\omega)+\mathcal{A}_{gh}^{LL}(\omega,\pi)\big]\big\}-V_{tb}V_{td}^*$$
$$\times\Big\{-\left(2a_3+a_4+2a_5+\frac{1}{2}a_7+\frac{1}{2}a_9-\frac{1}{2}a_{10}\right)\mathcal{A}_{ab}^{LL}(\omega,\pi)-\left(C_3+2C_4-\frac{1}{2}C_9+\frac{1}{2}C_{10}\right)\mathcal{A}_{cd}^{LL}(\omega,\pi)$$
$$-\left(2C_6+\frac{1}{2}C_8\right)\mathcal{A}_{cd}^{LR}(\omega,\pi)-\left(a_4+\frac{3}{2}a_7-\frac{3}{2}a_9-\frac{1}{2}a_{10}\right)\big[\mathcal{A}_{ab}^{LL}(\pi,\omega)+\mathcal{A}_{ef}^{LL}(\pi,\omega)+\mathcal{A}_{ef}^{LL}(\omega,\pi)\big]$$
$$-\left(C_3-\frac{1}{2}C_9-\frac{3}{2}C_{10}\right)\big[\mathcal{A}_{cd}^{LL}(\pi,\omega)+\mathcal{A}_{gh}^{LL}(\pi,\omega)+\mathcal{A}_{gh}^{LL}(\omega,\pi)\big]+\frac{3}{2}C_8\big[\mathcal{A}_{cd}^{LR}(\pi,\omega)+\mathcal{A}_{gh}^{LR}(\pi,\omega)+\mathcal{A}_{gh}^{LR}(\omega,\pi)\big]$$
$$-\left(a_6-\frac{1}{2}a_8\right)\big[\mathcal{A}_{ab}^{SP}(\pi,\omega)+\mathcal{A}_{ef}^{SP}(\pi,\omega)+\mathcal{A}_{ef}^{SP}(\omega,\pi)\big]-\left(C_5-\frac{1}{2}C_7\right)\big[\mathcal{A}_{cd}^{SP}(\pi,\omega)+\mathcal{A}_{cd}^{SP}(\omega,\pi)$$
$$+\mathcal{A}_{gh}^{SP}(\pi,\omega)+\mathcal{A}_{gh}^{SP}(\omega,\pi)\big]\Big\}\Big\},\tag{19}$$

In Fig. 5, we present the relationship between the invariant mass of the $\pi^+\pi^-$ pair and the CP asymmetry in the decay process $\bar{B}_d^0\to\pi^+\pi^-\pi^0$. Within a specific range of invariant masses, we observe a significant variation in the CP asymmetry within the $\rho^0-\omega-\phi$ mass region. The maximum value of CP asymmetry reaches 91%. Notably, slight peaks are observed at positions corresponding to the mass of the ϕ meson from Fig. 6.

To gain further insights into these observations, we investigate the impact of both three-particle and two-particle mixing effects on CP asymmetry in this decay process. By conducting regional integration analysis of CP and examining the resonance effects on CP asymmetry, we enhance our understanding of the contributions from different factors to variations in CP violation. Detailed discussions regarding this topic are presented in the subsequent section.

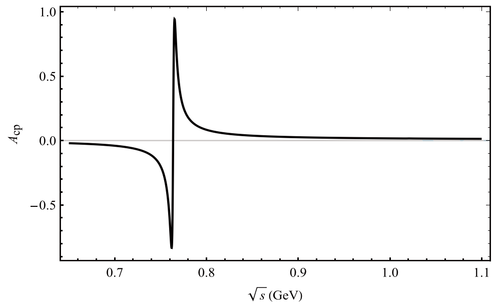

Fig. 5. Plot of $A_{\rm CP}$ as a function of $\sqrt{s}$ corresponding to central parameter values of CKM matrix elements for the decay channel of $\bar{B}_d^0\to\pi^+\pi^-\pi^0$.

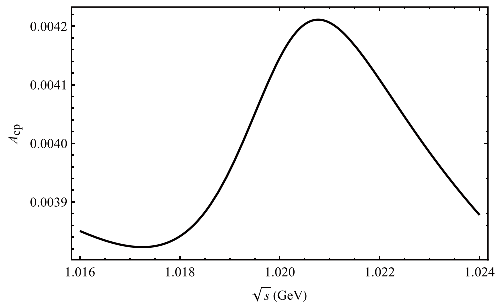

Fig. 6. CP asymmetry plot near the invariant mass of ϕ for the decay channel of $B_d^0\to\pi^+\pi^-\pi^0$ from the central parameter values of CKM matrix elements.

D. CP asymmetry analysis of the $\bar{B}_d^0\to(\rho^0,\omega,\phi\to\pi^+\pi^-)\bar{K}^0$ decay process

The above amplitude analysis investigates the impact of vector meson resonance effects on decay processes. During the decay process, vector meson resonances can induce the generation of strong phases. Different vector meson resonances can be observed to have varying effects on the CP asymmetry of decay processes. Investigating the resonance effect of vector mesons not only yields valuable physical insights into intermediate mesons in multi-body decay processes, but also presents a novel avenue for future experimental inquiries into CP asymmetry. Currently, there are no experimental data available on the $\bar{B}_d^0\to(\rho^0,\omega,\phi\to\pi^+\pi^-)\bar{K}^0$ decay process. We present the amplitude formulation of the $\bar{B}_d^0\to(\rho^0,\omega,\phi\to\pi^+\pi^-)\bar{K}^0$ decay process within the framework of PQCD. The three-body amplitude corresponding to diagram (a) of Fig. 1 can be expressed as follows:

$$A(a)=A(\overline{B}_d^0\to(\rho^0\to\pi^+\pi^-)\overline{K}^0)=\sum_{\lambda=0,\pm1}\frac{G_F P_{\bar{B}^0}\cdot\epsilon^*(\lambda)g^{\rho^0\to\pi^+\pi^-}\epsilon(\lambda)\cdot(p_{\pi^+}-p_{\pi^-})}{2(s-m_{\rho^0}^2+\mathrm{i}m_{\rho^0}\Gamma_{\rho^0})}$$

$$\times\left\{V_{ub}V_{us}^*\left\{a_2\left[\mathcal{A}_{ab}^{LL}(\rho,\overline{K})\right]+C_1\left[\mathcal{A}_{cd}^{LL}(\rho,\overline{K})\right]\right\}+\{V_{tb}V_{ts}^*\left\{\left(a_4-\frac{1}{2}a_{10}\right)\left[\mathcal{A}_{ab}^{LL}(\overline{K},\rho)+\mathcal{A}_{ef}^{LL}(\overline{K},\rho)\right]+\left(C_3-\frac{1}{2}C_9\right)\right.\right.$$
$$\times\left[\mathcal{A}_{cd}^{LL}(\overline{K},\rho)+\mathcal{A}_{gh}^{LL}(\overline{K},\rho)\right]+\left(a_6-\frac{1}{2}a_8\right)\left[\mathcal{A}_{ab}^{SP}(\overline{K},\rho)+\mathcal{A}_{ef}^{SP}(\overline{K},\rho)\right]+\left(C_5-\frac{1}{2}C_7\right)\left[\mathcal{A}_{cd}^{SP}(\overline{K},\rho)+\mathcal{A}_{gh}^{SP}(\overline{K},\rho)\right]$$
$$\left.\left.-\frac{3}{2}(a_7+a_9)\mathcal{A}_{ab}^{LL}(\rho,\overline{K})-\frac{3}{2}C_8\mathcal{A}_{cd}^{LR}(\rho,\overline{K})-\frac{3}{2}C_{10}\mathcal{A}_{cd}^{LL}(\rho,\overline{K})\right\}\right\}. \tag{20}$$

In Fig. 1, diagram (h) exhibits the resonance phenomenon between the ρ^0 meson and ω meson, along with the decay process of the ρ^0 meson into the pair of $\pi^+\pi^-$ mesons, which is indicated by black dots. Diagram (e) bears resemblance to diagram (h), yet it presents the decay process of the ρ^0 meson via the ϕ resonance. The amplitudes associated with diagrams (h) and (e) of Fig. 1 can be expressed as follows:

$$A(h)=A(\overline{B}_d^0\to(\omega-\rho^0\to\pi^+\pi^-)\overline{K}^0)=\sum_{\lambda=0,\pm1}\frac{G_FP_{\bar{B}^0}\cdot\epsilon^*(\lambda)\;g^{\rho^0\to\pi^+\pi^-}\epsilon(\lambda)\cdot(p_{\pi^+}-p_{\pi^-})}{2(s-m_{\rho^0}^2+\mathrm{i}m_{\rho^0}\Gamma_{\rho^0})(s-m_\omega^2+\mathrm{i}m_\omega\Gamma_\omega)}\tilde{\Pi}_{\rho^0\omega}$$
$$\times\left\{V_{ub}V_{us}^*\left\{a_2\left[\mathcal{A}_{ab}^{LL}(\omega,\overline{K})\right]+C_1\left[\mathcal{A}_{cd}^{LL}(\omega,\overline{K})\right]\right\}-\{V_{tb}V_{ts}^*\left\{(a_4-\frac{1}{2}a_{10})\left[\mathcal{A}_{ab}^{LL}(\overline{K},\omega)+\mathcal{A}_{ef}^{LL}(\overline{K},\omega)\right]+(C_3\right.\right.$$
$$-\frac{1}{2}C_9\Big)\left[\mathcal{A}_{cd}^{LL}(\overline{K},\omega)+\mathcal{A}_{gh}^{LL}(\overline{K},\omega)\right]+\left(a_6-\frac{1}{2}a_8\right)\left[\mathcal{A}_{ab}^{SP}(\overline{K},\omega)+\mathcal{A}_{ef}^{SP}(\overline{K},\omega)\right]+\left(C_5-\frac{1}{2}C_7\right)\left[\mathcal{A}_{cd}^{SP}(\overline{K},\omega)\right.$$
$$\left.\left.+\mathcal{A}_{gh}^{SP}(\overline{K},\omega)\right]+\left(2a_3+2a_5+\frac{1}{2}a_7+\frac{1}{2}a_9\right)\mathcal{A}_{ab}^{LL}(\omega,\overline{K})+(2C_4+\frac{1}{2}C_{10}\Big)\mathcal{A}_{cd}^{LL}(\omega,\overline{K})+\left(2C_6+\frac{1}{2}C_8\right)\mathcal{A}_{cd}^{LR}(\omega,\overline{K})\right\}\right\}, \tag{21}$$

$$A(e)=A(\overline{B}_d^0\to(\phi-\rho^0\to\pi^+\pi^-)\overline{K}^0)=\sum_{\lambda=0,\pm1}\frac{-G_FP_{\bar{B}^0}\cdot\epsilon^*(\lambda)\;g^{\rho^0\to\pi^+\pi^-}\epsilon(\lambda)\cdot(p_{\pi^+}-p_{\pi^-})}{\sqrt{2}(s-m_{\rho^0}^2+\mathrm{i}m_{\rho^0}\Gamma_{\rho^0})(s-m_\phi^2+\mathrm{i}m_\phi\Gamma_\phi)}\tilde{\Pi}_{\rho\phi}$$
$$\times\left\{V_{tb}V_{ts}^*\left\{\left(a_3+a_4+a_5-\frac{1}{2}a_7-\frac{1}{2}a_9-\frac{1}{2}a_{10}\right)\mathcal{A}_{ab}^{LL}(\phi,\overline{K})+\left(a_4-\frac{1}{2}a_{10}\right)\mathcal{A}_{ef}^{LL}(\phi,\overline{K})+\left(a_6-\frac{1}{2}a_8\right)\mathcal{A}_{ef}^{SP}(\phi,\overline{K})\right.\right.$$
$$+\left(C_3+C_4-\frac{1}{2}C_9-\frac{1}{2}C_{10}\right)\mathcal{A}_{cd}^{LL}(\phi,\overline{K})+\left(C_6-\frac{1}{2}C_8\right)\mathcal{A}_{cd}^{LR}(\phi,\overline{K})+\left(C_5-\frac{1}{2}C_7\right)\left[\mathcal{A}_{cd}^{SP}(\phi,\overline{K})+\mathcal{A}_{gh}^{SP}(\phi,\overline{K})\right]$$
$$\left.\left.+\left(C_3-\frac{1}{2}C_9\right)\mathcal{A}_{gh}^{LL}(\phi,\overline{K})\right\}\right\}. \tag{22}$$

The results of CP asymmetry for the $\bar{B}_d^0\to\pi^+\pi^-\bar{K}^0$ decay process are presented in Fig. 7. As depicted in Fig. 7, it is evident that the CP asymmetry of the $\bar{B}_d^0\to\pi^+\pi^-\bar{K}^0$ channel undergoes variations when the invariant masses of the pair of $\pi^+\pi^-$ mesons encompass the ranges corresponding to resonances such as ω and ϕ. Notably, a maximum CP asymmetry of -18% can be achieved.

The CP asymmetry in the decay process $\bar{B}_d^0\to\pi^+\pi^-\bar{K}^0$ exhibits a significant change when the invariant mass of the pair of $\pi^+\pi^-$ mesons approaches 0.75 GeV, reaching a peak value of -18%. This behavior can be attributed to the interference effect arising from the $\rho-\omega$ mixing mechanism, which is expected to occur within the range of 0.7−0.8 GeV. In addition, small peaks are observed in the invariant mass range corresponding to ϕ. In the decay

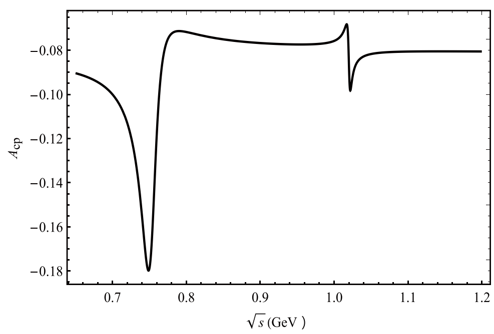

Fig. 7. Plot of A_{CP} as a function of $\sqrt{s}$ corresponding to central parameter values of CKM matrix elements for the decay channel of $\bar{B}_d^0\to\pi^+\pi^-\bar{K}^0$.

of $B_d^0 \to (\phi \to \pi^+\pi^-)\bar{K}^0$, penguin graph contributions play a significant role. Notably, the resonance effect arising from $\rho^0-\phi$ mixing exerts a substantial influence on CP asymmetry, resulting in an associated value of -9%.

IV. ANALYSIS OF REGIONAL CP ASYMMETRY IN THE DECAY PROCESS

The narrow width approximation (NWA) is employed in our calculation to decompose the three body decay process into two successive quasi-two-body decays: $B \to (R \to \pi^+\pi^-)P$, where R denotes the resonance state and P represents either a π or K meson. Considering the intermediate resonance state R, we introduce the correction factor η_R to define the expression

$$\eta_R = \frac{\mathcal{B}(B \to RP_3 \to P_1P_2P_3)}{\mathcal{B}(B \to RP_3)\mathcal{B}(R \to P_1P2)}, \tag{23}$$

which shows the relationship between the branch ratio measured around the resonance region and the branch ratio of the three-body decay of the B meson [38]. According to the QCDF method, the correction factor η_R is approximately 7% during the decay $B_u^- \to \pi^+\pi^-\pi^-$ [39, 40]. When calculating CP asymmetry, both the numerator and denominator contain the correction factor η_R, and they can cancel one another.

We investigate the resonant and non-resonant contributions within a specific region, examining how various particle resonances contribute to the CP asymmetry. Our calculations involve integrating the differential CP asymmetry parameter in both the numerator and denominator simultaneously, allowing us to derive regional CP asymmetry.

Theoretical errors can lead to uncertainty of the results in Table 2. The first error results from the variations in CKM parameters, and the second originates from hadronic parameters such as shape parameters, form factors, decay constants, and B meson wave functions. In Table 2, we present a comparison between our calculated results and the existing experimental data. Notably, intriguing observations of significant regional CP asymmetry have been reported in experiments conducted by the LHCb, BaBar, and Belle collaborations. Subsequently, we investigate the influence of different resonance effects on regional CP asymmetry. Owing to the close masses of the ρ^0 and ω mesons in these experiments, distinguishing between them becomes challenging. To address this issue, we incorporate this scenario into our calculations using the PQCD method within the resonance framework for decay channels such as $\bar{B}_d^0 \to \pi^+\pi^-\bar{K}^0$, $\bar{B}_d^0 \to \pi^+\pi^-\pi^0$, $B_u^- \to \pi^+\pi^-K^-$, and $B_u^- \to \pi^+\pi^-\pi^-$. Our results align with experimental error ranges, validating the accuracy of our calculation method. Specifically, in the decay channel of $\bar{B}_d^0 \to \pi^+\pi^-\bar{K}^0$, we observe that resonance contributions from three-particle mixtures significantly impact CP asymmetry.

In the decay process of $\bar{B}_d^0 \to \pi^+\pi^-\bar{K}^0$, a significant CP asymmetry value can be obtained by the intermediate ρ^0 meson. Considering the resonance effect of vector

Table 2. Peak regional $(0.70\,\text{GeV} \le \sqrt{s} \le 1.10\,\text{GeV})$ integral of A_{CP}^{Ω} from different resonance ranges for the $\bar{B}_d \to \pi^+\pi^-K^0$, $\bar{B}_d \to \pi^+\pi^-\pi^0$, $B_u^- \to \pi^+\pi^-K^-$, and $B_u^- \to \pi^+\pi^-\pi^-$ decay processes.

Decay channel	This work	Previous measurements (no mixing)
$\bar{B}_d^0 \to \pi^+\pi^-\bar{K}^0$	$-0.1683 \pm 0.0013 \pm 0.0000$ (ρ^0)	
	$-0.0847 \pm 0.0000 \pm 0.0084$ ($\rho^0-\omega$ mixing)	-----------------------------
	$-0.0813 \pm 0.0064 \pm 0.0052$ ($\rho^0-\phi$ mixing)	
	$-0.0847 \pm 0.0056 \pm 0.0089$ ($\phi-\rho^0-\omega$ mixing)	
$\bar{B}_d^0 \to \pi^+\pi^-\pi^0$	$-0.0054 \pm 0.0004 \pm 0.0011$ (ρ^0)	
	$0.0173 \pm 0.0109 \pm 0.0015$ ($\rho^0-\omega$ mixing)	-----------------------------
	$-0.0055 \pm 0.0006 \pm 0.0011$ ($\rho^0-\phi$ mixing)	
	$0.0147 \pm 0.0014 \pm 0.0086$ ($\phi-\rho^0-\omega$ mixing)	
$B_u^- \to \pi^+\pi^-K^-$	$0.2093 \pm 0.0206 \pm 0.0044$ (ρ^0)	0.150 ± 0.019 ± 0.011 LHCb [8]
	$0.1771 \pm 0.0084 \pm 0.0061$ ($\rho^0-\omega$ mixing)	0.44 ± 0.10 ± 0.04 BaBar [41]
	$0.2109 \pm 0.0207 \pm 0.0023$ ($\rho^0-\phi$ mixing)	0.30 ± 0.11 ± 0.02 Belle [42]
	$0.3470 \pm 0.0310 \pm 0.0709$ ($\phi-\rho^0-\omega$ mixing)	
$B_u^- \to \pi^+\pi^-\pi^-$	$0.0065 \pm 0.0014 \pm 0.0031$ (ρ^0)	-0.004 ± 0.017 ± 0.009 LHCb [8]
	$0.0256 \pm 0.0013 \pm 0.0016$ ($\rho^0-\omega$ mixing)	0.30 ± 0.11 ± 0.02 Belle [42]
	$0.0076 \pm 0.0006 \pm 0.0023$ ($\rho^0-\phi$ mixing)	
	$0.0260 \pm 0.0034 \pm 0.0047$ ($\phi-\rho^0-\omega$ mixing)	

mesons, the CP asymmetry value of three-body decay changes significantly. Combining the data in Table 2, the resonance effect plays a role in suppressing the CP asymmetry value of three-body decay. The suppression effects of two and three vector meson mixture resonances on the CP asymmetry value of the decay process are not significantly different.

In the decay process of $\bar{B}_d^0 \to \pi^+\pi^-\pi^0$, the mixed resonance effect of $\rho^0-\omega$ and $\phi-\rho^0-\omega$ makes a substantial contribution to CP asymmetry. The CP asymmetry value associated with the direct decay of the ρ^0 meson closely approximates the value obtained under the $\rho^0-\phi$ mixed resonance mechanism, indicating that this process is minimally affected by the presence of $\rho^0-\phi$ mixed resonance. Currently, there is a lack of experimental studies investigating the CP asymmetry in the $\bar{B}_d^0 \to \pi^+\pi^- K(\pi)$ three-body decay process. We anticipate that our prediction can serve as a valuable reference for future experiments.

The CP asymmetry value resulting from the intermediate ρ^0 meson in the $B_u \to \pi^+\pi^- K(\pi)$ decay process falls within the experimental error range. The decay process $B_u^- \to \pi^+\pi^- K^-$ exhibits a suppression effect owing to the presence of $\rho^0-\omega$ resonance, while significant contributions to CP asymmetry are observed from both the $\rho^0-\omega$ and $\phi-\rho^0-\omega$ resonances. Notably, the three-particle resonance contribution surpasses that of the $\rho^0-\phi$ mixed resonance in terms of CP asymmetry. In the decay process of $B_u^- \to \pi^+\pi^-\pi^-$, various mixed resonances have been considered in this study, leading to an overall enhancement in the CP asymmetry value. The contributions from the $\rho^0-\omega$ and $\phi-\rho^0-\omega$ mixed resonances are approximately equal in terms of CP asymmetry, while the mixing mechanism involving $\rho^0-\phi$ also contributes to CP asymmetry but with a smaller effect.

For vector particle resonances, the decay processes $\bar{B}_d \to \pi^+\pi^-\pi^0$ and $B_u^- \to \pi^+\pi^-\pi^-$ exhibit significant contributions to CP asymmetry compared with non-resonant decays. It is noteworthy that clear manifestations of CP asymmetry are observed within the resonance range. In the decay channel of $B_u^- \to \pi^+\pi^- K^-$, the resonance effects contribute more prominently to CP asymmetry, resulting in increased regional values similar to those observed in the decay channel $\bar{B}_d \to \pi^+\pi^- K^0$ within their respective invariant mass ranges.

V. SUMMARY AND DISCUSSION

We conducted a comprehensive analysis of the CP asymmetry in the three-body decay of the B meson, focusing specifically on regions of the invariant mass of the pair of $\pi^+\pi^-$ mesons. The research findings revealed an intriguing phenomenon: there are significant changes in CP asymmetry in different resonance regions (*e.g.*, resonances of the ρ^0, ω, and ϕ mesons). This finding suggests that these resonances play a significant role in influencing the decay dynamics and subsequent CP asymmetry. The presence of such distinct changes in CP asymmetry across different resonance regions provides valuable insights into our understanding of fundamental particle interactions. It highlights how specific energy regimes can affect particle decays and their associated symmetries.

We quantified the regional CP asymmetry by integrating over the phase space. In decays such as $\bar{B}_d^0 \to \pi^+\pi^-\bar{K}^0$, $\bar{B}_d^0 \to \pi^+\pi^-\pi^0$, $B_u^- \to \pi^+\pi^- K^-$, and $B_u^- \to \pi^+\pi^-\pi^-$, we observed CP asymmetry arising from contributions of two-meson and three-meson mixing processes. Notably, significant regional CP asymmetry was observed when involving $\rho^0-\phi-\omega$ mixing. Experimental detection of regional CP asymmetry can be achieved by reconstructing resonant states of the ρ^0, ω, and ϕ mesons within their respective resonance regions.

Recently, the LHCb experimental group has made significant progress in investigating the three-body decay of the B meson and has obtained noteworthy findings. By analyzing previous experimental data, they have measured direct CP asymmetry in various decay modes such as $B^\pm \to K^+K^-K^\pm$, $B^\pm \to \pi^+\pi^-K^\pm$, $B^\pm \to \pi^+\pi^-\pi^\pm$, and $B^\pm \to K^+K^-\pi^\pm$. Building upon the achievements of LHCb experiments, future investigations are expected to focus primarily on exploring the regional CP asymmetry of the three-body decays of the B meson in the resonance regions of ρ^0, ω, and ϕ mesons.

APPENDIX A: RELATED FUNCTIONS DEFINED IN THE TEXT

For ease of calculation, we define a scalar scale t and specify the concrete forms of some parameters, as follows:

$$
\begin{aligned}
t_{a,b}^V &= \max(\alpha_g^V, \beta_{a,b}^V, b_1, b_3), & \alpha_g^V &= m_B^2 x_1 x_3,\ \beta_a^V = m_B^2 x_3,\ \beta_b^V = m_B^2 x_1,\\
t_{c,d}^V &= \max(\alpha_g^V, \beta_{c,d}^V, b_2, b_3), & \alpha_g^V &= m_B^2 x_1 x_3,\ \beta_c^V = m_B^2 x_3 (x_1-\bar{x}_2),\ \beta_d^V = m_B^2 x_3 (x_1-x_2),\\
t_{c,d}^P &= \max(\alpha_g^P, \beta_{c,d}^P, b_2, b_3), & \alpha_g^P &= m_B^2 x_1 x_2,\ \beta_c^P = m_B^2 x_2 (x_1-\bar{x}_3),\ \beta_d^P = m_B^2 x_2 (x_1-x_3),\\
t_{e,f}^V &= \max(\alpha_a^V, \beta_{e,f}^V, b_2, b_3), & \alpha_a^V &= m_B^2 x_2 \bar{x}_3,\ \beta_e^V = m_B^2 \bar{x}_3,\ \beta_f^V = m_B^2 x_2,\\
t_{e,f}^P &= \max(\alpha_a^P, \beta_{e,f}^P, b_2, b_3), & \alpha_a^P &= m_B^2 \bar{x}_2 x_3,\ \beta_e^P = m_B^2 \bar{x}_2,\ \beta_f^P = m_B^2 x_3,
\end{aligned}
$$

$$t^V_{g,h} = \max(\alpha^V_a, \beta^V_{g,h}, b_1, b_2), \qquad \alpha^V_a = m_B^2 x_2 \bar{x}_3,\ \beta^V_g = \alpha^V_a - m_B^2 \bar{x}_1 (x_2 + \bar{x}_3),\ \beta^V_h = \alpha^V_a,\ -m_B^2 x_1 (x_2 + \bar{x}_3)$$
$$t^P_{g,h} = \max(\alpha^P_a, \beta^P_{g,h}, b_1, b_2), \qquad \alpha^P_a = m_B^2 \bar{x}_2 x_3,\ \beta^P_g = \alpha^P_a - m_B^2 \bar{x}_1 (\bar{x}_2 + x_3),\ \beta^P_h = \alpha^P_a - m_B^2 x_1 (\bar{x}_2 + x_3). \tag{A1}$$

Within the framework of PQCD, the non-perturbative part of the decay process is incorporated into the meson wave function. In this appendix, we present the expressions for the initial and final meson wave functions and the distribution amplitudes. The meson wave function should be a function related to k_T, and the B meson wave function can be expressed as [35, 43, 44, 45]

$$\Phi_B = \frac{i}{\sqrt{6}} (\not{P}_B + M_B) \gamma_5 \phi_B(x,b). \tag{A2}$$

In the above distribution amplitude $\phi_B(x,b)$, x represents the momentum fraction of the light quark in the B meson, and b represents the coordinate in the b space of the transverse momentum conjugate; its phenomenological expression for the distribution amplitude is

$$\phi_B(x,b) = N x^2 (1-x)^2 \exp\left\{-\left(\frac{x_1 m_B}{\sqrt{2}\omega_B}\right)^2 - \frac{1}{2}\omega_B^2 b^2\right\}, \tag{A3}$$

where $\omega_B$serves as a free parameter, and N acts as the normalization coefficient. In experiments involving B^0 and B^- mesons, ω_B is typically set to 0.4 ± 0.04 GeV. When $\omega_b = 0.4$ GeV, the normalization coefficient N yields a value of $N_B = 91.7456$ [46, 47]. The specific expression for the distribution amplitude of the final meson is as follows, where the vector meson V=ρ (ω or ϕ) [48, 49]: $\phi^t_V(x) = \frac{3f^T_V}{2\sqrt{6}} t^2$, $\phi^s_V(x) = \frac{3f^T_V}{2\sqrt{6}}(-t)$, $\phi^v_V(x) = \frac{3f_V}{8\sqrt{6}}(1+t^2)$, $\phi^a_V(x) = \frac{3f_V}{4\sqrt{6}}(-t)$, where $t = 2x-1$. Here, f_V and $f^{(T)}_V$ represent the decay constants for the longitudinal and transverse polarizations of vector mesons, respectively. The amplitude of the final-state distribution of scalar mesons is presented below. For the scalar meson P = π (K) [50],

$$\phi^A_p(x) = \frac{f_P}{\sqrt{6}} 3x(1-x)[1 + a^P_1 C^{3/2}_1(t) + a^P_2 C^{3/2}_2(t) + a^P_4 C^{3/2}_4(t)], \tag{A4}$$

$$\phi^P_p(x) = \frac{f_P}{2\sqrt{6}} \left[1 + \left(30\eta_3 - \frac{5}{2}\rho^2_P\right) C^{1/2}_2(t) - 3(\eta_3\omega_3 + \frac{9}{20}\rho^2_P(1+6a^p_2))C^{1/2}_4(t)\right], \tag{A5}$$

$$\phi^T_p(x) = \frac{f_P}{2\sqrt{6}}(1-2x)\left[1 + 6\left(5\eta_3 - \frac{1}{2}\eta_3\omega_3 - \frac{7}{20}\rho^2_P - \frac{3}{5}\rho^2_P a^P_2\right)(1-10x+10x^2)\right], \tag{A6}$$

where $t = 2x-1$, $\eta_3 = 0.015$, $\omega_3 = -3$, and the mass ratio $\rho_{\pi(K)} = m_{\pi(K)}/m^{(K)}_0$. The chiral scales are given by $m^\pi_0 = 1.4 \pm 0.3$ GeV and $m^K_0 = 1.6 \pm 0.1$ GeV, respectively. The Gegenbauer polynomials $C^\nu_n(t)$ are

$$C^{1/2}_2(t) = \frac{1}{2}(3t^2 - 1), \quad C^{1/2}_4(t) = \frac{1}{8}(+3 - 30t^2 + 35t^4),$$
$$C^{3/2}_2(t) = \frac{3}{2}(5t^2 - 1), \quad C^{3/2}_4(t) = \frac{15}{8}(1 - 14t^2 + 21t^4),$$
$$C^{3/2}_1(t) = 3t. \tag{A7}$$

The aggregated Gegenbauer moments a_i associated with the pertinent meson distribution amplitudes are expressed as

$$a^P_1 = C_2 + C_1/3, \quad a^P_2 = C_1 + C_2/3, \quad a^P_4 = C_4 + C_3/3. \tag{A8}$$

Here, ϕ^a_P and ϕ^v_V are the twist-2 wave functions, whereas $\phi^{p,t}_P$ and $\phi^{t,s}_V$ are the twist-3 wave functions. We provide specific expressions for the factorizable and non-factorizable amplitudes within PQCD, where $r_P = m_P/m_B$ and $r_V = m_V/m_B$.

We formally define $\mathcal{A}^k_{ij}(M_1, M_2) = \mathcal{A}^k_i(M_1, M_2) + \mathcal{A}^k_j(M_1, M_2)$. For the amplitude building block $\mathcal{A}^j_i(M_1, M_2)$, we employ the letter i to signify Feynman diagrams. Herein, (a) and (b) denote decomposable emission diagrams, (c) and (d) denote non-decomposable emission diagrams, (e) and (f) denote decomposable annihilation diagrams, and (g) and (h) denote non-factorized annihilation diagrams. We use the letter j to represent the three flow structures, namely $j = LL$ for $(V-A)\otimes(V-A)$, $j = LR$ for $(V-A)\otimes(V+A)$, and $j = SP$ for $-2(S-P)\otimes(S+P)$. The precise formulation of the constant C is presented below:

$$C = \frac{\pi C_F}{N_c^2} m_B^4 f_B f_P. \tag{A9}$$

After inserting the operators $j = LL$ for $(V-A)\otimes(V-A)$, $j = LR$ for $(V-A)\otimes(V+A)$, and $j = SP$ for $-2(S-P)\otimes(S+P)$, the decay amplitude contributions $\mathcal{A}^{LL}(P,V)$, $\mathcal{A}^{SP}(P,V)$, and $\mathcal{A}^{SP}(P,V)$ generated by the decomposable emission diagram can be expressed as follows:

$$\mathcal{A}_a^{LL}(P,V) = C\int \mathrm{d}x_1\,\mathrm{d}x_3\,\mathrm{d}b_1\,\mathrm{d}b_3\,H_{ab}(\alpha_g^V,\beta_a^V,b_1,b_3)\,\alpha_s(t_a^V)\,C_i(t_a^V)\left\{\phi_B\left[\phi_V^v(1+x_3)+\left(\phi_V^t+\phi_V^s\right)(\bar{x}_3-x_3)\right]\right\}, \tag{A10}$$

$$\mathcal{A}_a^{SP}(P,V) = C\int \mathrm{d}x_1\,\mathrm{d}x_3\,\mathrm{d}b_1\,\mathrm{d}b_3\,H_{ab}(\alpha_g^V,\beta_a^V,b_1,b_3)\,\alpha_s(t_a^V)\,C_i(t_a^V)2r_P\left\{\phi_B\left[-\phi_V^v+\phi_V^t x_3-\phi_V^s(2+x_3)\right]\right\}, \tag{A11}$$

$$\mathcal{A}_a^{LL}(V,P) = Cf_V^{\parallel}\int \mathrm{d}x_1\,\mathrm{d}x_2\,\mathrm{d}b_1\,\mathrm{d}b_2\,H_{ab}(\alpha_g^P,\beta_a^P,b_1,b_2)\,\alpha_s(t_a^P)\left\{\phi_B\left[\phi_P^a(1+x_2)+\left(\phi_P^p+\phi_P^t\right)(\bar{x}_2-x_2)\right]\right\}, \tag{A12}$$

$$\mathcal{A}_a^{SP}(V,P) = 0. \tag{A13}$$

$\mathcal{A}_a^{LL}(P,V)$ and $\mathcal{A}_b^{LL}(P,V)$ both represent amplitude contributions to the insertion of structure $(V-A)\otimes(V-A)$, but $\mathcal{A}_a^{LL}(P,V)$ and $\mathcal{A}_b^{LL}(P,V)$, as detailed in [51], correspond to different decay factorizable emission diagrams.

$$\mathcal{A}_b^{LL}(P,V) = 2C\int \mathrm{d}x_1\,\mathrm{d}x_3\,\mathrm{d}b_1\,\mathrm{d}b_3\,H_{ab}(\alpha_g^V,\beta_b^V,b_3,b_1)\,\alpha_s(t_b^V)\,C_i(t_b^V)\,S_t(x_1)\,\phi_B\,\phi_V^s, \tag{A14}$$

$$\mathcal{A}_b^{SP}(P,V) = -C\int \mathrm{d}x_1\,\mathrm{d}x_3\,\mathrm{d}b_1\,\mathrm{d}b_3\,H_{ab}(\alpha_g^V,\beta_b^V,b_3,b_1)\,\alpha_s(t_b^V)\,C_i(t_b^V)\,S_t(x_1)2r_P\left\{\phi_B\left[\phi_V^v x_1+2\phi_V^s\bar{x}_1\right]\right\}, \tag{A15}$$

$$\mathcal{A}_b^{LL}(V,P) = 2Cf_V^{\parallel}\int \mathrm{d}x_1\,\mathrm{d}x_2\,\mathrm{d}b_1\,\mathrm{d}b_2\,H_{ab}(\alpha_g^P,\beta_b^P,b_2,b_1)\,\alpha_s(t_b^P)\,C_i(t_b^P)\,S_t(x_1)\,\phi_B\,\phi_P^p. \tag{A16}$$

After inserting the three-stream structure, the amplitude contribution of the non-decomposable emission diagram is as follows:

$$\mathcal{A}_c^{LL}(P,V) = C\int \mathrm{d}x_1\,\mathrm{d}x_2\,\mathrm{d}x_3\,\mathrm{d}b_1\,\mathrm{d}b_2\,H_{cd}(\alpha_g^V,\beta_c^V,b_1,b_2)\,\alpha_s(t_c^V)\,C_i(t_c^V)\,S_t(x_3)\phi_P^a\left\{\phi_B\left[\phi_V^v(\bar{x}_2-x_1)+\left(\phi_V^t-\phi_V^s\right)x_3\right]\right\}_{b_1=b_3}, \tag{A17}$$

$$\mathcal{A}_c^{LR}(P,V) = C\int \mathrm{d}x_1\,\mathrm{d}x_2\,\mathrm{d}x_3\,\mathrm{d}b_1\,\mathrm{d}b_2\,H_{cd}(\alpha_g^V,\beta_c^V,b_1,b_2)\,\alpha_s(t_c^V)\,C_i(t_c^V)\,S_t(x_3)\phi_P^a\left\{\phi_B\left[\phi_V^v(x_1-\bar{x}_2)+\left(\phi_V^t+\phi_V^s\right)x_3-\phi_V^v x_3\right]\right\}_{b_1=b_3}, \tag{A18}$$

$$\begin{aligned}\mathcal{A}_c^{SP}(P,V) = C\int &\mathrm{d}x_1\,\mathrm{d}x_2\,\mathrm{d}x_3\,\mathrm{d}b_1\,\mathrm{d}b_2\,H_{cd}(\alpha_g^V,\beta_c^V,b_1,b_2)\,\alpha_s(t_c^V)\,C_i(t_c^V)\,S_t(x_3)\\ &\left\{\phi_B\left[\left(\phi_P^p+\phi_P^t\right)\left(\phi_V^v-\phi_V^t+\phi_V^s\right)(x_1-\bar{x}_2)-\left(\phi_P^p-\phi_P^t\right)\left(\phi_V^t+\phi_V^s\right)x_3\right]\right\}_{b_1=b_3},\end{aligned} \tag{A19}$$

$$\mathcal{A}_c^{LL}(V,P) = C\int \mathrm{d}x_1\,\mathrm{d}x_2\,\mathrm{d}x_3\,\mathrm{d}b_1\,\mathrm{d}b_3\,H_{cd}(\alpha_g^P,\beta_c^P,b_1,b_3)\,\alpha_s(t_c^P)\,C_i(t_c^P)\,S_t(x_2)\phi_V^v\left\{\phi_B\left[\phi_P^a(\bar{x}_3-x_1)-\left(\phi_P^p-\phi_P^t\right)x_2\right]\right\}_{b_1=b_2}, \tag{A20}$$

$$\mathcal{A}_c^{LR}(V,P) = C\int \mathrm{d}x_1\,\mathrm{d}x_2\,\mathrm{d}x_3\,\mathrm{d}b_1\,\mathrm{d}b_3\,H_{cd}(\alpha_g^P,\beta_c^P,b_1,b_3)\,\alpha_s(t_c^P)\,C_i(t_c^P)\,S_t(x_2)$$
$$\phi_V^v\left\{\phi_B\left[\phi_P^a(\bar{x}_3-x_1)-\left(\phi_P^p+\phi_P^t\right)x_2+\phi_P^a x_2\right]\right\}_{b_1=b_2}, \tag{A21}$$

$$\mathcal{A}_c^{SP}(V,P) = C\int \mathrm{d}x_1\,\mathrm{d}x_2\,\mathrm{d}x_3\,\mathrm{d}b_1\,\mathrm{d}b_3\,H_{cd}(\alpha_g^P,\beta_c^P,b_1,b_3)\,\alpha_s(t_c^P)\,C_i(t_c^P)\,S_t(x_2)$$
$$\left\{\phi_B\left[\left(\phi_P^a+\phi_P^p-\phi_P^t\right)\left(\phi_V^t+\phi_V^s\right)(\bar{x}_3-x_1)-\left(\phi_P^p+\phi_P^t\right)\left(\phi_V^t-\phi_V^s\right)x_2\right]\right\}_{b_1=b_2}, \tag{A22}$$

$$\mathcal{A}_d^{LL}(P,V) = C\int \mathrm{d}x_1\,\mathrm{d}x_2\,\mathrm{d}x_3\,\mathrm{d}b_1\,\mathrm{d}b_2\,H_{cd}(\alpha_g^V,\beta_d^V,b_1,b_2)\,\alpha_s(t_d^V)\,C_i(t_d^V)\,S_t(x_3)$$
$$\phi_p^a\left\{\phi_B\left[\phi_V^v(x_1-x_2)+\left(\phi_V^t+\phi_V^s\right)x_3-\phi_V^v x_3\right]\right\}_{b_1=b_3}, \tag{A23}$$

$$\mathcal{A}_d^{LR}(P,V) = C\int \mathrm{d}x_1\,\mathrm{d}x_2\,\mathrm{d}x_3\,\mathrm{d}b_1\,\mathrm{d}b_2\,H_{cd}(\alpha_g^V,\beta_d^V,b_1,b_2)\,\alpha_s(t_d^V)\,C_i(t_d^V)\,S_t(x_3)\phi_p^a\left\{\phi_B\left[\phi_V^v(x_2-x_1)+\left(\phi_V^t-\phi_V^s\right)x_3\right]\right\}_{b_1=b_3}, \tag{A24}$$

$$\mathcal{A}_d^{SP}(P,V) = C\int \mathrm{d}x_1\,\mathrm{d}x_2\,\mathrm{d}x_3\,\mathrm{d}b_1\,\mathrm{d}b_2\,H_{cd}(\alpha_g^V,\beta_d^V,b_1,b_2)\,\alpha_s(t_d^V)\,C_i(t_d^V)\,S_t(x_3)$$
$$\left\{\phi_B\left[\left(\phi_P^p-\phi_P^t\right)\left(\phi_V^v-\phi_V^t+\phi_V^s\right)(x_2-x_1)+\left(\phi_P^p+\phi_P^t\right)\left(\phi_V^t+\phi_V^s\right)x_3\right]\right\}_{b_1=b_3}, \tag{A25}$$

$$\mathcal{A}_d^{LL}(V,P) = C\int \mathrm{d}x_1\,\mathrm{d}x_2\,\mathrm{d}x_3\,\mathrm{d}b_1\,\mathrm{d}b_3\,H_{cd}(\alpha_g^P,\beta_d^P,b_1,b_3)\,\alpha_s(t_d^P)\,C_i(t_d^P)\,S_t(x_2)$$
$$\phi_V^v\left\{\phi_B\left[\phi_P^a(x_1-x_3)+\left(\phi_P^p+\phi_P^t\right)x_2-\phi_P^a x_2\right]\right\}_{b_1=b_2}, \tag{A26}$$

$$\mathcal{A}_d^{LR}(V,P) = C\int \mathrm{d}x_1\,\mathrm{d}x_2\,\mathrm{d}x_3\,\mathrm{d}b_1\,\mathrm{d}b_3\,H_{cd}(\alpha_g^P,\beta_d^P,b_1,b_3)\,\alpha_s(t_d^P)\,C_i(t_d^P)\,S_t(x_2)\phi_V^v\left\{\left(\phi_B\left[\phi_P^a(x_1-x_3)+\left(\phi_P^p-\phi_P^t\right)x_2\right]\right\}_{b_1=b_2}, \tag{A27}$$

$$\mathcal{A}_d^{SP}(V,P) = C\int \mathrm{d}x_1\,\mathrm{d}x_2\,\mathrm{d}x_3\,\mathrm{d}b_1\,\mathrm{d}b_3\,H_{cd}(\alpha_g^P,\beta_d^P,b_1,b_3)\,\alpha_s(t_d^P)\,C_i(t_d^P)\,S_t(x_2)$$
$$\left\{\phi_B\left[\left(\phi_P^a+\phi_P^p-\phi_P^t\right)\left(\phi_V^t-\phi_V^s\right)(x_3-x_1)-\left(\phi_P^p+\phi_P^t\right)\left(\phi_V^t+\phi_V^s\right)x_2\right]\right\}_{b_1=b_2}, \tag{A28}$$

In the factorizable annihilation diagrams, the amplitude contributions of $(V-A)\otimes(V-A)$, $(V-A)\otimes(V+A)$, and $-2(S-P)\otimes(S+P)$ are as follows:

$$\mathcal{A}_e^{LL}(P,V) = C\int \mathrm{d}x_2\,\mathrm{d}x_3\,\mathrm{d}b_2\,\mathrm{d}b_3\,H_{ef}(\alpha_a^V,\beta_e^V,b_2,b_3)\,\alpha_s(t_e^V)\,C_i(t_e^V)\left\{2\phi_P^p\left[\phi_V^t x_3+\phi_V^s(1+\bar{x}_3)\right]-\phi_P^a\phi_V^v\bar{x}_3\right\}S_t(\bar{x}_3), \tag{A29}$$

$$\mathcal{A}_e^{SP}(P,V) = 2C\int \mathrm{d}x_2\,\mathrm{d}x_3\,\mathrm{d}b_2\,\mathrm{d}b_3\,H_{ef}(\alpha_a^V,\beta_e^V,b_2,b_3)\,\alpha_s(t_e^V)C_i(t_e^V)\,S_t(\bar{x}_3)\left\{\phi_P^a\left(\phi_V^t+\phi_V^s\right)\bar{x}_3-2\phi_P^p\phi_V^v\right\}, \tag{A30}$$

$$\mathcal{A}_e^{LL}(V,P) = -C\int \mathrm{d}x_2\,\mathrm{d}x_3\,\mathrm{d}b_2\,\mathrm{d}b_3\,H_{ef}(\alpha_a^P,\beta_e^P,b_3,b_2)\,\alpha_s(t_e^P)\,C_i(t_e^P)\left\{\phi_P^a\phi_V^v\bar{x}_2+2\phi_V^s\left[\phi_P^p(1+\bar{x}_2)+\phi_P^t x_2\right]\right\}S_t(\bar{x}_2), \tag{A31}$$

$$\mathcal{A}_e^{SP}(V,P) = 2C\int \mathrm{d}x_2\,\mathrm{d}x_3\,\mathrm{d}b_2\,\mathrm{d}b_3\,H_{ef}(\alpha_a^P,\beta_e^P,b_3,b_2)\,\alpha_s(t_e^P)C_i(t_e^P)\,S_t(\bar{x}_2)\left\{2\phi_P^a\phi_V^s+\phi_V^v\left(\phi_P^p+\phi_P^t\right)\bar{x}_2\right\}, \tag{A32}$$

$$\mathcal{A}_f^{LL}(P,V) = C\int \mathrm{d}x_2\,\mathrm{d}x_3\,\mathrm{d}b_2\,\mathrm{d}b_3\,H_{ef}(\alpha_a^V,\beta_f^V,b_3,b_2)\,\alpha_s(t_f^V)\,C_i(t_f^V)\left\{\phi_P^a\phi_V^v x_2-2\phi_V^s\left[\phi_P^p(1+x_2)-\phi_P^t\bar{x}_2\right]\right\}S_t(x_2), \tag{A33}$$

$$\mathcal{A}_f^{SP}(P,V) = 2C\int \mathrm{d}x_2\,\mathrm{d}x_3\,\mathrm{d}b_2\,\mathrm{d}b_3\,H_{ef}(\alpha_a^V,\beta_f^V,b_3,b_2)\,\alpha_s(t_f^V)C_i(t_f^V)\,S_t(x_2)\left\{2\,\phi_P^a\phi_V^s - \left(\phi_P^p-\phi_P^t\right)\phi_V^v\,x_2\right\}, \tag{A34}$$

$$\mathcal{A}_f^{LL}(V,P) = C\int \mathrm{d}x_2\,\mathrm{d}x_3\,\mathrm{d}b_2\,\mathrm{d}b_3\,H_{ef}(\alpha_a^P,\beta_f^P,b_2,b_3)\,\alpha_s(t_f^P)\,C_i(t_f^P)\left\{\phi_P^a\phi_V^v\,x_3 - 2\,\phi_P^p\left[\phi_V^t\,\bar{x}_3 - \phi_V^s\,(1+x_3)\right]\right\}S_t(x_3), \tag{A35}$$

$$\mathcal{A}_f^{SP}(V,P) = 2C\int \mathrm{d}x_2\,\mathrm{d}x_3\,\mathrm{d}b_2\,\mathrm{d}b_3\,H_{ef}(\alpha_a^P,\beta_f^P,b_2,b_3)\,\alpha_s(t_f^P)C_i(t_f^P)\,S_t(x_3)\left\{2\,\phi_P^p\phi_V^v - \phi_P^a\left(\phi_V^t-\phi_V^s\right)x_3\right\}, \tag{A36}$$

In an irreducible annihilation diagram, all three wave functions are involved. The decay amplitudes for the three types of processes take the following forms:

$$\begin{aligned}\mathcal{A}_g^{LL}(P,V) = C\int &\mathrm{d}x_1\,\mathrm{d}x_2\,\mathrm{d}x_3\,\mathrm{d}b_1\,\mathrm{d}b_2\,H_{gh}(\alpha_a^V,\beta_g^V,b_1,b_2)\,\alpha_s(t_g^V)\,C_i(t_g^V)\left\{\phi_B\left[\left(\phi_P^p\phi_V^t-\phi_P^t\phi_V^s\right)(\bar{x}_3-x_2) - \phi_P^a\phi_V^v\,(x_1+x_2)\right.\right.\\ &\left.\left.+\left(\phi_P^p\phi_V^s-\phi_P^t\phi_V^t\right)(x_2+\bar{x}_3-2\,\bar{x}_1)+4\,\phi_P^p\phi_V^s\right]\right\}_{b_2=b_3},\end{aligned} \tag{A37}$$

$$\begin{aligned}\mathcal{A}_g^{LR}(P,V) = C\int &\mathrm{d}x_1\,\mathrm{d}x_2\,\mathrm{d}x_3\,\mathrm{d}b_1\,\mathrm{d}b_2\,H_{gh}(\alpha_a^V,\beta_g^V,b_1,b_2)\,\alpha_s(t_g^V)\,C_i(t_g^V)\left\{\phi_B\left[\left(\phi_P^p\phi_V^t-\phi_P^t\phi_V^s\right)(\bar{x}_3-x_2) + \phi_P^a\phi_V^v\,(x_1+\bar{x}_3)\right.\right.\\ &\left.\left.-\left(\phi_P^p\phi_V^s-\phi_P^t\phi_V^t\right)(x_2+\bar{x}_3-2\,\bar{x}_1)-4\,\phi_P^p\phi_V^s\right]\right\}_{b_2=b_3},\end{aligned} \tag{A38}$$

$$\begin{aligned}\mathcal{A}_g^{SP}(P,V) = C\int &\mathrm{d}x_1\,\mathrm{d}x_2\,\mathrm{d}x_3\,\mathrm{d}b_1\,\mathrm{d}b_2\,H_{gh}(\alpha_a^V,\beta_g^V,b_1,b_2)\,\alpha_s(t_g^V)\,C_i(t_g^V)\left\{\phi_B\left[\phi_P^a\left(\phi_V^t-\phi_V^s\right)(x_3-x_1) - \left(\phi_P^p+\phi_P^t\right)\phi_V^v\right.\right.\\ &\left.\left.+\phi_P^a\left(\phi_V^t-\phi_V^s\right)+\left(\phi_P^p+\phi_P^t\right)\phi_V^v\,(x_2-\bar{x}_1)\right]\right\}_{b_2=b_3},\end{aligned} \tag{A39}$$

$$\begin{aligned}\mathcal{A}_g^{LL}(V,P) = C\int &\mathrm{d}x_1\,\mathrm{d}x_2\,\mathrm{d}x_3\,\mathrm{d}b_1\,\mathrm{d}b_3\,H_{gh}(\alpha_a^P,\beta_g^P,b_1,b_3)\,\alpha_s(t_g^P)\,C_i(t_g^P)\left\{\phi_B\left[\left(\phi_P^p\phi_V^t-\phi_P^t\phi_V^s\right)(\bar{x}_2-x_3) - \phi_P^a\phi_V^v\,(x_1+x_3)\right.\right.\\ &\left.\left.-\left(\phi_P^p\phi_V^s-\phi_P^t\phi_V^t\right)(\bar{x}_2+x_3-2\,\bar{x}_1)-4\,\phi_P^p\phi_V^s\right]\right\}_{b_2=b_3},\end{aligned} \tag{A40}$$

$$\begin{aligned}\mathcal{A}_g^{LR}(V,P) = C\int &\mathrm{d}x_1\,\mathrm{d}x_2\,\mathrm{d}x_3\,\mathrm{d}b_1\,\mathrm{d}b_3\,H_{gh}(\alpha_a^P,\beta_g^P,b_1,b_3)\,\alpha_s(t_g^P)\,C_i(t_g^P)\left\{\phi_B\left[\left(\phi_P^p\phi_V^t-\phi_P^t\phi_V^s\right)(\bar{x}_2-x_3) + \phi_P^a\phi_V^v\,(x_1+\bar{x}_2)\right.\right.\\ &\left.\left.+\left(\phi_P^p\phi_V^s-\phi_P^t\phi_V^t\right)(\bar{x}_2+x_3-2\,\bar{x}_1)+4\,\phi_P^p\phi_V^s\right]\right\}_{b_2=b_3},\end{aligned} \tag{A41}$$

$$\begin{aligned}\mathcal{A}_g^{SP}(V,P) = C\int &\mathrm{d}x_1\,\mathrm{d}x_2\,\mathrm{d}x_3\,\mathrm{d}b_1\,\mathrm{d}b_3\,H_{gh}(\alpha_a^P,\beta_g^P,b_1,b_3)\,\alpha_s(t_g^P)\,C_i(t_g^P)\left\{\phi_B\left[\phi_P^a\left(\phi_V^t+\phi_V^s\right)(\bar{x}_1-x_3) - \left(\phi_P^p-\phi_P^t\right)\phi_V^v\right.\right.\\ &\left.\left.+\phi_P^a\left(\phi_V^t+\phi_V^s\right)+\left(\phi_P^p-\phi_P^t\right)\phi_V^v\,(x_1-x_2)\right]\right\}_{b_2=b_3},\end{aligned} \tag{A42}$$

$$\begin{aligned}\mathcal{A}_h^{LL}(P,V) = C\int &\mathrm{d}x_1\,\mathrm{d}x_2\,\mathrm{d}x_3\,\mathrm{d}b_1\,\mathrm{d}b_2\,H_{gh}(\alpha_a^V,\beta_h^V,b_1,b_2)\,\alpha_s(t_h^V)\,C_i(t_h^V)\left\{\phi_B\left[\left(\phi_P^p\phi_V^t-\phi_P^t\phi_V^s\right)(\bar{x}_3-x_2) + \phi_P^a\phi_V^v\,(\bar{x}_3-x_1)\right.\right.\\ &\left.\left.-\left(\phi_P^p\phi_V^s-\phi_P^t\phi_V^t\right)(x_2+\bar{x}_3-2\,x_1)\right]\right\}_{b_2=b_3},\end{aligned} \tag{A43}$$

$$\begin{aligned}\mathcal{A}_h^{LR}(P,V) = C\int &\mathrm{d}x_1\,\mathrm{d}x_2\,\mathrm{d}x_3\,\mathrm{d}b_1\,\mathrm{d}b_2\,H_{gh}(\alpha_a^V,\beta_h^V,b_1,b_2)\,\alpha_s(t_h^V)\,C_i(t_h^V)\left\{\phi_B\left[\left(\phi_P^p\phi_V^t-\phi_P^t\phi_V^s\right)(\bar{x}_3-x_2) + \phi_P^a\phi_V^v\,(x_1-x_2)\right.\right.\\ &\left.\left.+\left(\phi_P^p\phi_V^s-\phi_P^t\phi_V^t\right)(x_2+\bar{x}_3-2\,x_1)\right]\right\}_{b_2=b_3},\end{aligned} \tag{A44}$$

$$\begin{aligned}\mathcal{A}_h^{SP}(P,V) = C\int &\mathrm{d}x_1\,\mathrm{d}x_2\,\mathrm{d}x_3\,\mathrm{d}b_1\,\mathrm{d}b_2\,H_{gh}(\alpha_a^V,\beta_h^V,b_1,b_2)\,\alpha_s(t_h^V)\,C_i(t_h^V)\left\{\phi_B\left[\left(\phi_P^p+\phi_P^t\right)\phi_V^v\,(x_1-x_2) + \phi_P^a\left(\phi_V^t-\phi_V^s\right)\right.\right.\\ &\left.\left.(\bar{x}_3-x_1)\right]\right\}_{b_2=b_3},\end{aligned} \tag{A45}$$

$$\mathcal{A}_h^{LL}(V,P) = C\int \mathrm{d}x_1\,\mathrm{d}x_2\,\mathrm{d}x_3\,\mathrm{d}b_1\,\mathrm{d}b_3\,H_{gh}(\alpha_a^P,\beta_h^P,b_1,b_3)\,\alpha_s(t_h^P)\,C_i(t_h^P)\Big\{\phi_B\Big[\big(\phi_P^p\phi_V^t-\phi_P^t\phi_V^s\big)(\bar{x}_2-x_3)+\phi_P^a\phi_V^v(\bar{x}_2-x_1)$$
$$+\big(\phi_P^p\phi_V^s-\phi_P^t\phi_V^t\big)(\bar{x}_2+x_3-2x_1)\Big]\Big\}_{b_2=b_3}, \tag{A46}$$

$$\mathcal{A}_h^{LR}(V,P) = C\int \mathrm{d}x_1\,\mathrm{d}x_2\,\mathrm{d}x_3\,\mathrm{d}b_1\,\mathrm{d}b_3\,H_{gh}(\alpha_a^P,\beta_h^P,b_1,b_3)\,\alpha_s(t_h^P)\,C_i(t_h^P)\Big\{\phi_B\Big[\big(\phi_P^p\phi_V^t-\phi_P^t\phi_V^s\big)(\bar{x}_2-x_3)+\phi_P^a\phi_V^v(x_1-x_3)$$
$$-\big(\phi_P^p\phi_V^s-\phi_P^t\phi_V^t\big)(\bar{x}_2+x_3-2x_1)\Big]\Big\}_{b_2=b_3}, \tag{A47}$$

$$\mathcal{A}_h^{SP}(V,P) = C\int \mathrm{d}x_1\,\mathrm{d}x_2\,\mathrm{d}x_3\,\mathrm{d}b_1\,\mathrm{d}b_3\,H_{gh}(\alpha_a^P,\beta_h^P,b_1,b_3)\,\alpha_s(t_h^P)\,C_i(t_h^P)$$
$$\Big\{\phi_B\Big[\big(\phi_P^p-\phi_P^t\big)\phi_V^v(x_1-\bar{x}_2)+\phi_P^a\big(\phi_V^t+\phi_V^s\big)(x_3-x_1)\Big]\Big\}_{b_2=b_3}. \tag{A48}$$

The function H is derived from the Fourier transform of the function H^0 [52], and these definitions are as follows:

$$H_{ab}(\alpha,\beta,b_i,b_j) = b_i b_j K_0\big(b_i\sqrt{\alpha}\big)\Big\{\theta\big(b_i-b_j\big)K_0\big(b_i\sqrt{\beta}\big)I_0\big(b_j\sqrt{\beta}\big)+\big(b_i\leftrightarrow b_j\big)\Big\}, \tag{A49}$$

$$N_c H_{cd}(\alpha,\beta,b_1,b_i) = b_1 b_i\Big\{\theta(b_1-b_2)K_0\big(b_1\sqrt{\alpha}\big)I_0\big(b_i\sqrt{\alpha}\big)+\big(b_1\leftrightarrow b_i\big)\Big\}$$
$$\Big\{\theta(\beta)K_0\big(b_i\sqrt{\beta}\big)+\mathrm{i}\frac{\pi}{2}\theta(-\beta)\Big[J_0\big(b_i\sqrt{-\beta}\big)+\mathrm{i}\,Y_0\big(b_i\sqrt{-\beta}\big)\Big]\Big\}, \tag{A50}$$

$$H_{ef}(\alpha,\beta,b_i,b_j) = -\frac{\pi^2}{4}b_i b_j\Big\{J_0\big(b_i\sqrt{\alpha}\big)+\mathrm{i}\,Y_0\big(b_i\sqrt{\alpha}\big)\Big\}$$
$$\Big\{\theta\big(b_i-b_j\big)\Big[J_0\big(b_i\sqrt{\beta}\big)+\mathrm{i}\,Y_0\big(b_i\sqrt{\beta}\big)\Big]J_0\big(b_j\sqrt{\beta}\big)+\big(b_i\leftrightarrow b_j\big)\Big\}, \tag{A51}$$

$$N_c H_{gh}(\alpha,\beta,b_1,b_i) = b_1 b_i\Big\{\frac{\mathrm{i}\pi}{2}\theta(\beta)\Big[J_0\big(b_1\sqrt{\beta}\big)+\mathrm{i}\,Y_0\big(b_1\sqrt{\beta}\big)\Big]+\theta\big(-\beta\big)K_0\big(b_1\sqrt{-\beta}\big)\Big\}$$
$$\frac{\mathrm{i}\pi}{2}\Big\{\theta\big(b_1-b_i\big)\Big[J_0\big(b_1\sqrt{\alpha}\big)+\mathrm{i}\,Y_0\big(b_1\sqrt{\alpha}\big)\Big]J_0\big(b_i\sqrt{\alpha}\big)+\big(b_1\leftrightarrow b_i\big)\Big\}. \tag{A52}$$

References

[1] L. B. Okun, Sov. Phys. Usp. **9**, 574 (1967)
[2] M. E. Shaposhnikov, Phys. Lett. B **277**, 324 (1992)
[3] A. Alavi-Harati *et al.* (KTeV), Phys. Rev. Lett. **84**, 408 (2000)
[4] K. Abe *et al.* (Belle), Phys. Rev. Lett. **87**, 091802 (2001)
[5] B. Aubert *et al.* (BaBar), Phys. Rev. D **65**, 051101 (2002)
[6] N. Cabibbo, Phys. Rev. Lett. **10**, 531 (1963)
[7] R. Aaij *et al.* (LHCb), Phys. Rev. Lett. **124**, 031801 (2020)
[8] R. Aaij *et al.* (LHCb), Phys. Rev. D **108**, 012013 (2023)
[9] M. Kobayashi and T. Maskawa, Prog. Theor. Phys. **49**, 652 (1973)
[10] R. Aaij *et al.* (LHCb), Phys. Rev. Lett. **111**, 101801 (2013)
[11] R. Aaij *et al.* (LHCb), Phys. Rev. Lett. **112**, 011801 (2014)
[12] R. Aaij *et al.* (LHCb), Phys. Rev. D**90**, 112004 (2014)
[13] H. Y. Cheng, C. K. Chua and Z. Q. Zhang, Phys. Rev. D **94**, 094015 (2016)
[14] J. J. Qi, Z. Y. Wang, X. H. Guo *et al.*, Nucl. Phys. B **948**, 114788 (2019)
[15] J. J. Qi, Z. Y. Wang and X. H. Guo, Nucl. Phys. B **989**, 116132 (2023)
[16] X. L. Yuan, G. Lü, N. Wang *et al.*, Chin. Phys. C **47**, 113101 (2023)
[17] T. Huber, S. Kränkl and X. Q. Li, JHEP **2016**, 112 (2016)
[18] D. S. Shi, G. Lü, Y. L. Zhao *et al.*, Eur. Phys. J. C **83**, 345 (2023)
[19] Gang. L, Y. Lu, S.-T. Li *et al.*, Eur. Phys. J. C **77**, 518 (2017)
[20] G. Lü, C. C. Zhang, Y. L. Zhao *et al.*, Chin. Phys. C **48**, 013103 (2024)
[21] Q. Chang, L. Yang, Z. T. Zou *et al.*, Eur. Phys. J. C **84**, 753 (2024)
[22] M. Beneke, P. Böer, P. Rigatos *et al.*, Eur. Phys. J. C **81**, 638 (2021)
[23] J. Hua, H. N. Li, C. D. Lu *et al.*, Phys. Rev. D **104**, 016025 (2021)
[24] Y. Yang, X. Zhao, L. Lang *et al.*, Chin. Phys. C **46**, 083103 (2022)
[25] Gang. L, Y.-L. Zhao, L.-C. Liu *et al.*, Chin. Phys. C **46**, 113101 (2022)
[26] A. Ali, G. Kramer, and C. D. Lü, Phys. Rev. D **58**, 094009 (1998); **59**, 014005 (1998); Y. H. Chen, H. Y. Cheng, B. Tseng *et al.*, Phys. Rev. D **60**, 094014 (1999)

[27] C. E. Wolfe, K. Maltman, Phys. Rev. D **80**, 114024 (2009)
[28] M. N. Achasov, et.al., Nucl. Phys. B **569**, 158 (2000)
[29] T. N. Pham, Nucl. Phys. B Proc. Suppl. **163**, 35 (2007)
[30] A. Gordon *et al*. [Belle], Phys. Lett. B **542**, 183 (2002)
[31] C. P. Jessop *et al*. [CLEO], Phys. Rev. Lett. **85**, 2881 (2000)
[32] L. Wolfenstein, Phys. Rev. Lett. **51**, 1945 (1983); Phys. Rev. Lett. **13**, 562 (1964)
[33] H. Y. Cheng and C. K. Chua, Phys. Rev. D **102**, 053006 (2020)
[34] C. H. Chen and H. N. Li, Phys. Lett. B **561**, 258 (2003)
[35] Y. Li, C. D. Lu, Z. J. Xiao *et al*., Phys. Rev. D **70**, 034009 (2004)
[36] S. Navas *et al*. [Particle Data Group], Phys. Rev. D **110**, 030001 (2024)
[37] H. n. Li and S. Mishima, Phys. Rev. D **74**, 094020 (2006)
[38] C. K. Chua, H. Y. Cheng and C. W. Chiang, PoS **EPS-HEP2021**, 506 (2022)
[39] H. Y. Cheng, Phys. Rev. D **106**, 113004 (2022)
[40] H. Y. Cheng, C. W. Chiang and C. K. Chua, Phys. Lett. B **813**, 136058 (2021)
[41] B. Aubert *et al*. [BaBar], Phys. Rev. D **78**, 012004 (2008)
[42] A. Garmash *et al*.[Belle], Phys. Rev. Lett. **96**, 251803 (2006)
[43] J. J. Wang, D. T. Lin, W. Sun *et al*., Phys. Rev. D **89**, 074046 (2014)
[44] Y. Y. Keum, H. N. Li and A. I. Sanda, Phys. Rev. D **63**, 054008 (2001)
[45] A. Ali, G. Kramer, Y. Li *et al*., Phys. Rev. D **76**, 074018 (2007)
[46] Y. Y. Keum, H. N. Li, and A. I. Sanda, Phys. Lett. B **504**, 6 (2001); Phys. Rev. D **63**, 054008 (2001)
[47] C.D. Lü, K. Ukai, and M.-Z. Yang, Phys. Rev. D **63**, 074009 (2001)
[48] P. Ball and V. M. Braun, Nucl. Phys. B **543**, 201 (1999)
[49] P. Ball and R. Zwicky, Phys. Rev. D **71**, 014029 (2005)
[50] Xin Liu, Zhen-Jun Xiao, and Cai-Dian Lü, Phys. Rev. D **81**, 014022 (2010)
[51] Y. Yang, L. Lang, X. Zhao *et al*., Phys. Rev. D **103**, 056006 (2021)
[52] D. Q. Guo, X. F. Chen and Z. J. Xiao, Phys. Rev. D **75**, 054033 (2007)